UNIVERSITY OF CALIFORNIA
RIVERSIDE

Dissociative Energy Transfer for Probing Structural Details of Biomolecules in the Gas-Phase

A Dissertation submitted in partial satisfaction
of the requirements for the degree of

Doctor of Philosophy

in

Chemistry

by

Nathan Gardner Hendricks

August 2016

Dissertation Committee:
Dr. Ryan Julian, Chairperson
Dr. Cynthia Larive
Dr. Huiwang Ai

The Dissertation of Nathan Gardner Hendricks is approved:

_____

_____

_____

Committee Chairperson

University of California, Riverside

Acknowledgements

I would like to thank the many people who have supported me throughout the years in my pursuit of higher education. I would like thank all of my family, especially my mother Kathy and my aunt Wendy who have always been ready to help and support me when I needed it the most. I thank Alexandra Muir, who has always been by my side with patience, support, and love.

I want to thank all my coworkers and peers in the Julian lab who have aided me through my graduate career through discussion, advice, training, or direct collaboration: James Bonner, Lance Talbert, Dylan Riggs, Yana Lyon, Chris Nellessen, Thu Huong Pham, Yuanqi Tao, Xing Zhang, Omar Hamdy, Benjamin Moore, Arun Agarwal, Arman Alizadeh, and Neil Quebbemann. Also thanks to our collaborators in John McLean's group at Vanderbilt University: Nichole Lareau and Sarah Stow, who worked with us on the research presented in chapter 2.

I would also like to give special thanks to my mentors at University of California, San Diego: Professor Pieter Dorrestein, Dr. Yongxuan Su, and Professor Seth Cohen, who gave me opportunities, training, and encouragement that has been incredibly influential in my education and career path.

Finally, I thank my dissertation advisor, Ryan Julian, who has been my mentor at University of California, Riverside. Ryan has guided my research and intellectual development through countless hours of meetings, advice, training, and interaction.

I also acknowledge funding from the National Science Foundation, UC Riverside, and the American Society for Mass Spectrometry which has made my graduate education possible.

Text in this dissertation is reprinted with permission from the following publications:

1 N. G. Hendricks, N. M. Lareau, S. M. Stow, J. A. McLean and R. R. Julian, *J. Am. Chem. Soc.*, 2014, **136**, 13363–13370.

2 N. G. Hendricks and R. R. Julian, *Phys. Chem. Chem. Phys.*, 2015, **17**, 25822–7.

3 N. G. Hendricks and R. R. Julian, *Chem. Commun.*, 2015, **51**, 12720–3.

Dedication

To my father, Randy Hendricks

ABSTRACT OF THE DISSERTATION

Dissociative Energy Transfer for Probing Structural Details of Biomolecules in the Gas-Phase

by

Nathan Gardner Hendricks

Doctor of Philosophy, Graduate Program in Chemistry
University of California, Riverside, August 2016
Dr. Ryan R. Julian, Chairperson

The structure of biomolecules is of fundamental importance to their function and activity. Proteins and peptides adopt three-dimensional conformations that affect every facet of their role in biology ranging from stability, solubility, catalytic and enzymatic interactions, function and dysfunction. These structures are not easily predicted through their primary sequence of amino acids, and there is a strong desire to develop methods for identifying the conformation of biomolecules so that we can better understand biology, disease, and the spectrum of topics and applications that stem from these things. The work embodied in this document represents efforts to build tools that allow us to decipher these structures.

Disulfides can be utilized as receptors for energy transfer from nearby chromophores. The chromophores capable of acting as energy transfer donors include the tyrosine and tryptophan sidechains. Together, this system presents an elegant method to exploit already-present protein chemical moieties in proteins to perform distance-sensitive energy transfer experiments which form the foundation of this work. The excited state of a disulfide bond is a dissociative state, meaning that an intermolecular disulfide receiving energy transfer will result in a mass loss that is detectable by mass spectrometry. This phenomenon is explored in detail, and utilized to extract distance constraints within biomolecular structures. This system, referred to as action-excitation energy transfer (action-EET), is applied to the study of peptides structure, protein structure, and the effects of various conditions such as electrospray solvent on structure. Details about the local solvation environment of the donor chromophore, and special cases such as two-step energy transfer can also be inferred from the action-EET spectra, yielding even more highly specific information that be utilized in structural characterization. This information is then used to guide computations of biomolecule structure to relevant structures to obtain plausible, experimentally-corroborated simulations that are stronger than a purely computational approach. Together, this work presents a useful method for exploring the structure of gaseous biomolecules, as well as a foundation to develop future work in gaseous ion spectroscopy related to energy transfer.

Table of Contents

List of Figures

List of Tables

List of Schemes

Chapter 1: Introduction

Enhancing our abilities for characterizing the three-dimensional structures of biomolecules has been a growing focus in the field of mass spectrometry. Proteins adopt folded structures in the solution phase which are not easily predicted by their primary sequence of amino acids. The collective impact of secondary, tertiary, and quaternary structure affects every facet of a protein's function in biology. Accordingly, gaining an understanding of protein structure is a central task in the understanding of many biological phenomena.

1.1 Methods for Structural Characterization of Biomolecules

Currently, X-ray crystallography represents one of the principle methods for structural characterization of proteins. This method provides detailed structural information on the arrangement of atoms within a crystallized sample. One major limitation of this method is the difficulty in obtaining suitable crystals for analysis. The amount of protein necessary for crystal formation is typically large and prohibitive to the analysis of many proteins of interest. Additionally, not all proteins will crystallize to form suitable samples for characterization. Finally, it has been noted that in some cases the structure represented in the crystal is not reflective of that which is observed in solution.[1] While still highly informative, and often held as the "gold standard" for protein structure elucidation, it is clear that X-ray crystallography is not sufficient to analyze all structures.

Nuclear magnetic resonance (NMR) is also used for the characterization of protein structure. While highly established and versatile as a characterization tool for small molecules, NMR has also found use in the analysis of various small proteins. Analysis of

NMR data becomes increasingly complex as the size of the molecule increases. The end result is that NMR is generally relegated to the analysis of smaller sequences, although multi-dimensional NMR experiments, isotope labelling, and other techniques have enabled analysis of large proteins in various cases.[2] While the application of NMR to larger structures is a constantly developing area, it is still currently limited by the large amounts of sample required for the experiments. Both NMR and X-ray crystallography share this common obstacle, rendering these methods inapplicable to many low abundance or hard-to-isolate proteins. This creates significant limitations in our ability to structurally characterize newly-discovered proteins, biomolecules, and complexes of interest, many of which are hard to obtain in large quantity.

1.2 Mass Spectrometry in Structural Characterization

The limitations of currently established methods for structural determination of proteins has led interest in developing mass spectrometry-based techniques for this purpose. Mass spectrometry has been established as a major player in the field of proteomics. Its speed, sensitivity, and online compatibility with separations techniques render it ideal for the analysis of low-abundance proteins in mixtures and digests and high-throughput applications. With the sensitivity and viability of mass spectrometry for protein analysis well-established, there has been growing effort in leveraging mass spectrometry for the use in structural characterization. While not immediately obvious how mass spectrometry can be of value as a structural probe where the data obtained is a mass-to-charge ratio, various techniques have shown that more information can be extracted from these experiments. For instance, it has been shown that the charge state distribution of proteins reflects the

unfolding or retention of globular or even native structures.[3,4] Conventional understanding of this phenomenon suggests that highly charged states are denatured primarily as a result of high coulombic repulsion, whereas lower charge states may retain a globular or even native form. Combining solution phase experiments with mass spectrometry also enables the extraction of structural information, such as is the case with chemical crosslinking experiments or H/D exchange.[5] In chemical crosslinking, a protein or some such structure is modified covalently with a crosslinking agent which attaches to two or more sites in the protein (typically amines). The protein can then be digested and analyzed by mass spectrometry. The fragment peptides will contain a number of peptides covalently linked by the crosslinking agent, giving some information as to which residues are solvent accessible and near in space in the solution structure.[6,7] In H/D exchange, fast-exchanging protons on a protein are swapped out with deuterium in deuterated solvent. The mass shift from the deuterium can then be detected by mass spectrometry to gauge the solvent exposure of particular peptides and fragments, yielding useful structure information.[8] H/D exchange reactions have also been done in the gas phase to probe gaseous structure.[9]

While the previously mentioned techniques represent methods for structural determination that generally utilize an unmodified mass spectrometer, a great deal more can be achieved by augmenting the instrument. Ion mobility is frequently paired with mass spectrometry (IMS-MS) to yield conformer-selected separation of ions in the gas phase. In ion mobility, ions are separated in a gas-filled drift tube by their collisional cross sections (CCS), which are dependent on the conformation of the ion. The number of collisions an ion incurs as it travels through the drift gas is proportional to its arrival time, hence differing

CCS's can be correlated with arrival time.[10] Studies can then calculate the expected CCS of an ion and compare it to the observed IMS data. Studies with IMS-MS have looked at protein structure, amyloid formation, peptide structure, and many other systems of biological interest.[11-14]

While the utility of IMS-MS for separating conformers is well demonstrated, there are certain limitations of the method which create pitfalls for its use in structure elucidation. The output obtained from IMS is a single value that collectively represents the overall cross section of a molecule. As such, obtaining any specific structural details is dubious with IMS. Furthermore, differing structures can have similar or identical CCS values which complicate interpretation of the data. This issue is further complicated by imperfections in the methods for calculating a predicted cross section, and varying degrees of resolving power in IMS instruments. The end result is that many potential structures may fit the data after accounting for the limitations involved in collecting and interpreting IMS-MS.

1.3 Spectroscopy-Coupled Mass Spectrometry

Another modification to mass spectrometers of increasing popularity is the addition of a laser enabling photodissociation (PD) or action spectroscopy experiments. PD experiments involve coupling a laser with (typically) an ion trap instrument so ions can be held, photo-excited, then analyzed by MS (see figure 1.1). The application of these experiments have been numerous, including 193 nm and 213 nm UV dissociation for protein fragmentation,[15] 266 nm UV dissociation for site-selective radical fragmentation,[16,17] and multi-wavelength IR dissociation to generate action spectra.[18]

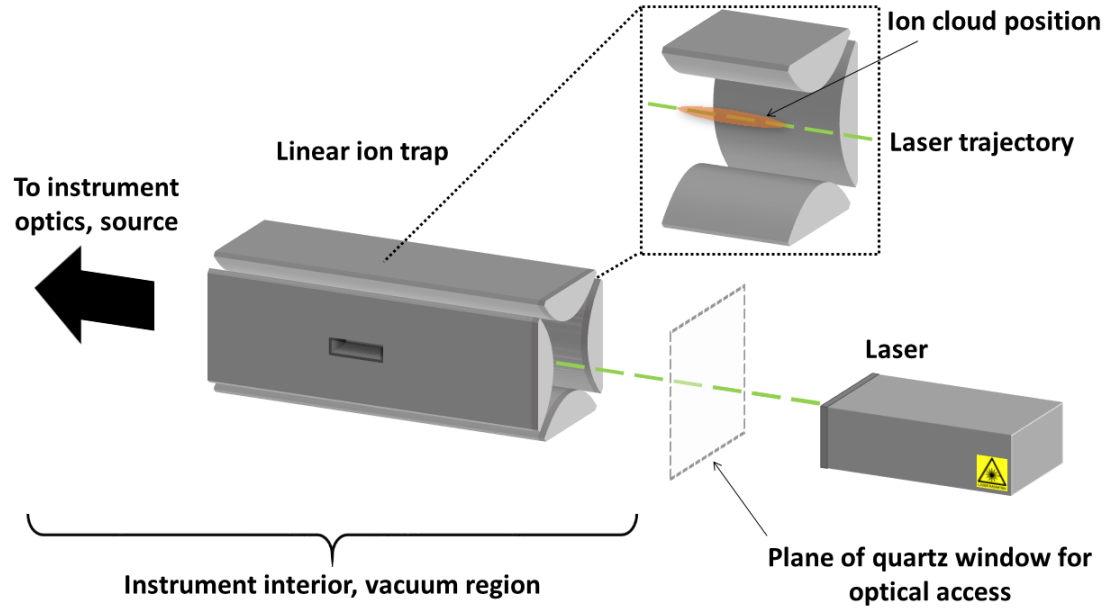

Figure 1.1. Sample schematic diagram showing the configuration of a linear ion trap instrument that allows laser excitation of ions.

266 nm UV dissociation has been used extensively in the Julian lab, particularly for dissociation of carbon-iodine bonds. The carbon-iodine bond cleaves homolytically under excitation to generate a radical at that site which can be further activated with CID to promote migration and radical dissociation pathways. The advantages of such dissociation experiments are that the radical initiation site is specific and migration pathways to initiate fragmentation are limited to areas that are near in space to that site. The result is that radical-directed dissociation (RDD) is structurally sensitive and can yield information about the conformers of gaseous molecules, as has been shown with ubiquitin, the KIX protein, and other systems.[17,16,19,20]

Spectroscopy-coupled mass spectrometry experiments present another subfield of growing interest for structurally sensitive technique development. Action spectroscopy

experiments, where lasers are used to fragment molecules and the resulting mass loss is measured by mass spectrometry as a function of wavelength, have existed for some time.[21-24] These types of action spectroscopy experiments enable the exploration of UV and IR spectral properties of ions in the gas phase. Infrared multi-photon dissociation (IRMPD) is one of the more prominent techniques in action spectroscopy. Studies have been performed with IRMPD to assign structures to a number of systems ranging from reaction intermediates, metallated ions, radical ions, and other systems.[25-27]

1.4 Gaseous Energy Transfer Experiments

An emerging area of interest is utilizing energy transfer systems for spectroscopy-coupled mass spectrometry experiments. An energy transfer experiment utilizes one-or-more donor chromophores which is excited at a specific wavelength, and an acceptor chromophore which can receive energy transfer from the excited donor over limited distances. Such energy transfer systems are useful for determining distance constraints within three-dimensional structure. Forster Resonance Energy Transfer (FRET) has been utilized extensively in the solution phase to study changes in protein conformation, molecular recognition, enzymatic pathways, and many other aspects of biology.[28-30] FRET is a non-radiative dipole-dipole interaction between two chromophores with spectral overlap which dominates at larger distances of separation (exceeding 20 Å).[31,32] The intensity of energy transfer decays according to $1/r^6$, with r being the distance between the donor and acceptor, giving rise to the transfer of energy over relatively large distances (see scheme 1.1 for the FRET equation). FRET represents the most frequently cited form of energy transfer, however other mechanisms for energy transfer exist. At shorter distances,

other mechanisms of energy transfer are more prominent. Namely, Dexter energy transfer is the primary form of energy transfer at distances shorter than 20 Å.[32] Dexter energy transfer, in contrast to FRET, is an electron exchange between two chromophores with spectral overlap, and the rate of energy transfer decays exponentially with distance between the chromophores (as can be seen in scheme 1.2). For practical purposes, these mechanisms are hard to distinguish from each other outside of the distance regimes at which they operate and the mathematical dependence of their energy transfer rates. For inclusiveness and accuracy, the term Excitation Energy Transfer (EET) is used to refer to the combination of mechanisms that result in energy transfer.

$$E = \frac{1}{1 + \left(\frac{r}{R_0}\right)^6}$$

Scheme 1.1. The FRET equation where E is the FRET efficiency, r is the donor-acceptor separation, and R0 is the Förster distance for the donor-acceptor pair, or the distance at which FRET efficiency is half.

$$k_{dexter} = KJe^{\frac{-2R_{DA}}{L}}$$

Scheme 1.2. The Dexter Energy Transfer equation, where k_{dexter} is the rate of energy transfer, J is the normalized spectral overlap integral, K is an experimentally determined factor, R_{DA} is the donor-acceptor distance, and L is the sum of the van der Waals radii.

Naturally, extending from the current applications of spectroscopy in mass spectrometry, there has been a desire to perform energy transfer experiments in mass spectrometers. Energy transfer experiments present a method capable of giving highly specific information about structures in the gas phase, which has been a long sought-after goal as mentioned previously. There have been a small number of attempts to combine

traditional FRET experiments with mass spectrometry. Typically, FRET is monitored by observing fluorescence from the acceptor chromophore after selective excitation of the donor chromophore, indication energy has been transferred from one to the other. Monitoring fluoresce in solution-phase experiments is generally trivial, but there are significant complications when attempting this inside a mass spectrometer. First, the instrument must be modified to allow both initial excitation and observation of the ion cloud. Excitation of ions can be achieved easily with linear ion trap mass spectrometers, but observation of the ions must be orthogonal to excitation which necessitates significant modification of the instrument. Second, the number of ions present in the ion cloud of a mass spectrometer is far below the desirable number of ions for observing fluorescence. Accordingly, these types of experiments encounter substantial sensitivity hurdles.

Despite these obstacles, a select few groups have achieved various successes with these types of traditional FRET experiments in the gas phase. The Parks group performed FRET experiments in the gas phase examining oligonucleotides, polypeptides, and the Trp-cage miniprotein.[33-35] Following Parks, Zenobi was also able to observe gas-phase FRET[36,37] and Jockusch has had success with the application of these FRET experiments to peptides and proteins.[38,39] These forays into gas-phase FRET have relied on established donor-acceptor pairs that are well-studied in solution, such as BODIPY-TMR and BODIPY-TR.[34] An additional challenge of these applications of FRET is that the spectroscopic properties of these chromophores and energy transfer systems do not translate directly to the gas phase. While using these known systems serves as a strong starting point for delving into

the gas-phase, it is clear that a great deal about the properties of these systems needs to be re-learned.[40,41]

Given the technical challenges of applying a traditional FRET system to gas-phase studies, it has long been recognized that an energy transfer donor-acceptor pair that indicates energy transfer through a mass change rather than fluorescence would be ideal. Such system would be analogous to action spectroscopy, where the spectroscopy of ions is elegantly probed through dissociation-induced mass losses that are measured directly by mass spectrometry, removing the hurdles associated with measuring fluorescence in a mass spectrometer. In this ideal system, a donor chromophore would absorb a photon at a particular wavelength, transfer energy (when near enough) to a special acceptor chromophore which would then undergo an excited state dissociation pathway to yield a specific mass loss that indicates energy transfer has occurred. While a system such as this has been sought after, no such suitable system had been characterized until very recently.

The challenges of developing a functional action-energy transfer system lie largely in the difficulty of finding a suitable acceptor for these experiments. As mentioned above, the acceptor must have an excited state dissociation pathway to be useful for this application. The reason for this is that typical chromophores will relax from excitation by internal conversion, leading to a distribution of vibrational energy across the molecule that results in fragmentation. This internal conversion forms the foundation for most action spectroscopy experiments, however the fragments yielded from this process are the same regardless of what chromophore has been excited; this means that this fragmentation pathway cannot be used to distinguish whether energy transfer has occurred in a system or

not. By contrast, a chromophore with an excited state dissociation pathway will have a unique fragmentation product, meaning that it can easily be determined if energy has been transferred to such an acceptor chromophore. Further complicating the search for a suitable acceptor, many of the photochemical properties for systems studied in solution change when transferred to the gas phase.[40,41]

The work in this dissertation covers the characterization and development of an action energy transfer system, as well as the application of this technique to various systems. This system, called Action-excitation energy transfer (Action-EET), utilizes a disulfide bond as an acceptor and tryptophan or tyrosine as donors.

1.5 Scope of dissertation

Chapter 2 describes chemistry that enables excitation energy transfer (EET) to be accurately measured via action spectroscopy on gaseous ions in an ion trap. It is demonstrated that EET between tryptophan or tyrosine and a disulfide bond leads to excited state, homolytic fragmentation of the disulfide bond. This phenomenon exhibits a tight distance dependence, which is consistent with Dexter exchange transfer. The extent of fragmentation of the disulfide bond can be used to determine the distance between the chromophore and disulfide bond. The chemistry is well suited for the examination of protein structure in the gas phase since native amino acids can serve as the donor/acceptor moieties. Furthermore, both tyrosine and tryptophan exhibit unique action spectra, meaning that the identity of the donating chromophore can be easily determined in addition to the distance between donor/acceptor. Application of the method to the Trpcage miniprotein reveals distance constraints that are consistent with a native-like fold for the

+2 charge state in the gas phase. This structure is stabilized by several salt-bridges, which have also been observed to be important previously in proteins that retain native-like structures in the gas phase. The ability of this method to measure specific distance constraints, potentially at numerous positions if combined with site-directed mutagenesis, significantly enhances our ability to examine protein structure in the gas phase.

In chapter 3, action-EET is combined with molecular dynamics calculations to rapidly and accurately reveal gaseous peptide structures. Three peptides in various charge states are examined. The influence of increasing charge state on peptide structure is easily observed. The presence of multiple conformations can be detected. Furthermore, the method is demonstrated to aid the assignment of charge, which is frequently nontrivial for peptides containing numerous acidic and basic residues that could adopt a variety of conformers of equal charge state. Comparison with ion mobility reveals that many low energy structures that are distinguishable by distance constraints would not be resolvable by collision cross section. Action-EET is demonstrated to be a powerful new tool for structure elucidation.

Chapter 4 explores gaseous two-step energy transfer, a potentially useful phenomenon for exploring macromolecular structure. Single step EET is observed for tyrosine and tryptophan containing peptides, but not for phenylalanine. Herein, we report sequential energy transfer from phenylalanine to tyrosine to a disulfide, resulting in homolytic cleavage of a sulfur-sulfur bond. Interestingly, energy transfer from phenylalanine is only observed in the presence of tyrosine and only occurs within certain distance constraints. Isolated, electronically excited phenylalanine is known to have an extremely long lifetime

in the gas phase, potentially suggesting quicker relaxation occurs via energy transfer to tyrosine. Alternatively, the direct overlap of states between phenylalanine and disulfide bonds is predicted to be poor, in which case tyrosine would serve to bridge the gap. In either case, the distance constraints imposed by this two-step EET are shown to be useful for evaluation and determination of gaseous biomolecular structure.

1.6 References

[1]D. R. Cooper, P. J. Porebski, M. Chruszcz and W. Minor, *Expert Opin. Drug Discov.*, 2011, **6**, 771–782.
[2]J. Fiaux, E. B. Bertelsen, A. L. Horwich and K. Wüthrich, *Nature*, 2002, **418**, 207–11.
[3]S. K. Chowdhury, V. Katta and B. T. Chait, *J. Am. Chem. Soc.*, 1990, **112**, 9012–9013.
[4]J. A. Loo, R. R. O. Loo, H. R. Udseth, C. G. Edmonds and R. D. Smith, *Rapid Commun. Mass Spectrom.*, 1991, **5**, 101–105.
[5]J. G. Mandell, A. M. Falick and E. A. Komives, *Anal. Chem.*, 1998, **70**, 3987–3995.
[6]A. Sinz, *Mass Spectrom. Rev.*, 2006, **25**, 663–82.
[7]J. Seebacher, P. Mallick, N. Zhang, J. S. Eddes, R. Aebersold and M. H. Gelb, *J. Proteome Res.*, 2006, **5**, 2270–82.
[8]L. Konermann, J. Pan and Y.-H. Liu, *Chem. Soc. Rev.*, 2011, **40**, 1224–34.
[9]J. H. Stewart, R. H. Shapiro, C. H. DePuy and V. M. Bierbaum, *J. Am. Chem. Soc.*, 1977, **99**, 7650–7653.
[10]T. Wyttenbach and M. T. Bowers, in *Modern Mass Spectrom.*, 2003, vol. 225, pp. 207–232.
[11]S. L. Bernstein, N. F. Dupuis, N. D. Lazo, T. Wyttenbach, M. M. Condron, G. Bitan, D. B. Teplow, J.-E. Shea, B. T. Ruotolo, C. V Robinson and M. T. Bowers, *Nat. Chem.*, 2009, **1**, 326–31.
[12]B. C. Bohrer, S. I. Merenbloom, S. L. Koeniger, A. E. Hilderbrand and D. E. Clemmer, *Annu. Rev. Anal. Chem.*, 2008, **1**, 293–327.
[13]T. Wyttenbach and M. T. Bowers, in *Modern Mass Spectrom.*, 2003, vol. 225, pp. 207–232.
[14]S. R. Harvey, C. E. Macphee and P. E. Barran, *Methods*, 2011, **54**, 454–61.
[15]J. S. Brodbelt, *Chem. Soc. Rev.*, 2014, **43**, 2757–83.
[16]T. Ly and R. R. Julian, *J. Am. Chem. Soc.*, 2010, **132**, 8602–9.
[17]T. Ly and R. R. Julian, *J. Am. Chem. Soc.*, 2008, **130**, 351–8.
[18]N. C. Polfer, *Chem. Soc. Rev.*, 2011, **40**, 2211–21.
[19]X. Zhang and R. R. Julian, *Int. J. Mass Spectrom.*, 2011, **308**, 225–231.

[20]B. B. Kirk, A. J. Trevitt, S. J. Blanksby, Y. Tao, B. N. Moore and R. R. Julian, *J. Phys. Chem. A*, 2013, **117**, 1228–32.
[21]R. C. Dunbar, *Int. J. Mass Spectrom.*, 2000, **200**, 571–589.
[22]T. D. Fridgen, *Mass Spectrom. Rev.*, **28**, 586–607.
[23]J. Roithová, *Chem. Soc. Rev.*, 2012, **41**, 547–59.
[24]N. C. Polfer and J. Oomens, *Mass Spectrom. Rev.*, **28**, 468–94.
[25]J. Roithová, *Chem. Soc. Rev.*, 2012, **41**, 547–59.
[26]N. C. Polfer, B. Paizs, L. C. Snoek, I. Compagnon, S. Suhai, G. Meijer, G. von Helden and J. Oomens, *J. Am. Chem. Soc.*, 2005, **127**, 8571–9.
[27]C. L. Moss, J. Chamot-Rooke, E. Nicol, J. Brown, I. Campuzano, K. Richardson, J. P. Williams, M. F. Bush, B. Bythell, B. Paizs and F. Turecek, *J. Phys. Chem. B*, 2012, **116**, 3445–56.
[28]K. Deuschle, *Plant Cell Online*, 2006, **18**, 2314–2325.
[29]R. Roy, S. Hohng and T. Ha, *Nat. Methods*, 2008, **5**, 507–16.
[30] T. Rantanen, M.-L. Järvenpää, J. Vuojola, K. Kuningas and T. Soukka, *Angew. Chemie*, 2008, **120**, 3871–3873.
[31]A. Periasamy, *J. Biomed. Opt.*, 2001, **6**, 287–91.
[32]J. R. Winkler, *Science*, 2013, **339**, 1530–1.
[33]A. T. Iavarone, A. Patriksson, D. van der Spoel and J. H. Parks, *J. Am. Chem. Soc.*, 2007, **129**, 6726–6735.
[34]A. S. Danell and J. H. Parks, *J. Am. Soc. Mass Spectrom.*, 2003, **14**, 1330–9.
[35]A. T. Iavarone and J. H. Parks, *J. Am. Chem. Soc.*, 2005, **127**, 8606–8607.
[36]M. Dashtiev, V. Azov, V. Frankevich, L. Scharfenberg and R. Zenobi, *J. Am. Soc. Mass Spectrom.*, 2005, **16**, 1481–7.
[37]V. Frankevich, V. Chagovets, F. Widjaja, K. Barylyuk, Z. Yang and R. Zenobi, *Phys. Chem. Chem. Phys.*, 2014, **16**, 8911–20.
[38]F. Talbot, A. Rullo, H. Yao and R. A. Jockusch, *J. Am. Chem. Soc.*, 2010, 16156–16164.
[39]M. F. Czar, F. Zosel, I. König, D. Nettels, B. Wunderlich, B. Schuler, A. Zarrine-Afsar and R. A. Jockusch, *Anal. Chem.*, 2015, **87**, 7559–65.
[40]M. W. Forbes and R. a Jockusch, *J. Am. Soc. Mass Spectrom.*, 2011, **22**, 93–109.
[41]S. Daly, A. Kulesza, G. Knight, L. MacAleese, R. Antoine and P. Dugourd, *J. Phys. Chem. A*, 2015, **119**, 5634–41.

Chapter 2: Bond Specific Dissociation following Excitation Energy Transfer for Distance Constraint Determination in the Gas Phase

2.1 Introduction

Meaningful examination of protein structure in the gas phase is complicated by several fundamental challenges. Perhaps most obviously, the gas phase is a foreign environment where proteins are not typically found. Indeed, intact transfer of proteins into the gas phase proved to be a challenge for some time, and the eventual solutions to this problem were recognized with Nobel prizes.[1,2] Subsequent improvements in speed and sensitivity have now made mass spectrometry (MS) the method of choice for protein identification and sequencing.[3] For these same reasons, considerable effort is currently being employed to develop methods that can extract information about protein structure in the gas phase.[4] However, our understanding of how proteins are transferred into the gas phase and how this process impacts structure is both imperfect and rapidly evolving. Important factors to be considered include the instrument/source conditions and relevant timescales over which protein structure can be preserved. Although it is clear that significant features of solution phase protein structure can be retained in the gas phase in some cases,[5,6] there are also examples where solution phase structure appears to be lost.[7,8]

Ion mobility is the most commonly implemented experimental technique for examining protein structure in the gas phase.[9] Although ion mobility provides direct measurement of the overall collision cross-section of a protein, no specific information about sub-structural

elements is revealed. It can be difficult to confidently discriminate numerous structural possibilities with this type of global structural information. Recent experiments relying on radical based chemistry have helped to provide more specific information about the distances between particular residues. For example, radicals can easily be generated at specific sites with atomic precision in proteins. Subsequently, radical directed dissociation (which typically takes place at different sites than where the initial radical was created) can easily be monitored by mass spectrometry. In this fashion, distance constraints between the initial and final radical positions can be estimated.[5,7] Similarly, MS/MS experiments and ion/molecule reactions can be used to probe the probability of recombination of two radicals created at two separate, specific sites.[10] Although these experiments provide detailed sub-structural information, the difficulty with these methods is that radical migration within a protein is not easily modeled or a function of any simple chemical or physical property.

An alternative way of probing specific distances (and thus structural features) in proteins relies on excitation energy transfer (EET).[11] EET encompasses a number of mechanisms including Dexter energy transfer and more popularly, Förster resonance energy transfer (FRET). FRET is notable for the transfer of energy at distances which can exceed 40 angstroms, making it a valuable tool for examining protein conformation, enzymatic activity, metabolic pathways, and many other aspects of biology where distance probes are useful.[12-15] Dexter energy transfer or Dexter exchange transfer is also a distance-sensitive form of EET that requires overlapping orbitals between chromophores and results from the synchronous exchange of two electrons.[16] Due to the requirement that molecular orbitals

must overlap, Dexter energy transfer occurs at much shorter distances than are typically associated with FRET. Additionally, the distance dependence for Dexter energy transfer is exponential, and is rarely observed to occur at distances over 15 angstroms.[11]

The implementation of traditional EET based methods in gas phase experiments is difficult. Both the number of ions that can be interrogated in gas phase experiments and optical access to them make direct observation of emission difficult to achieve. Nevertheless, a few groups have succeeded with the traditional approach.[17-26] Similar challenges exist for gas phase spectroscopy experiments, which led to the development of action spectroscopy.[27] In these experiments fragmentation, which is easily and sensitively measured by a mass spectrometer, is monitored rather than absorption or emission. In theory, a similar scheme should work for EET, where photon absorption would occur at one chromophore, followed by energy transfer and fragmentation at the other. There is a subtle (but very important) difference between action EET and action spectroscopy, namely, for action EET to work, energy transfer must lead to excitation of a dissociative excited state[28,29] in the acceptor. The reason for this requirement is simple. If dissociation occurred following internal conversion of the energy into vibrational excitation, then intramolecular vibrational energy redistribution would lead to identical products whether energy conversion occurred in the donor or the acceptor. Therefore, no characteristic peaks would be generated that would uniquely indicate energy transfer. On the other hand, if excitation of the donor leads to specific fragmentation of the acceptor prior to internal conversion, then energy transfer is straightforwardly identified.

In the solution phase, previous studies have found that disulfide reduction by UV is enhanced by the presence of tryptophan.[30] Additional studies have found disulfides to participate in photochemical reactions in conjunction with tryptophan.[31] Accordingly there is some evidence that disulfides may participate with tryptophan in EET. However, to the best of our knowledge, no such investigation has been performed on the gas phase chemistry of this system.

In this work, we reveal an EET pair suitable for action spectroscopy. It is demonstrated that excitation of tryptophan/tyrosine leads to direct dissociation of proximal disulfide bonds. Spectra for the tryptophan, disulfide, tryptophan/disulfide, and tyrosine/disulfide pairs are reported in the range of 250-300nm and confirm that energy transfer occurs, followed by excited state fragmentation. The distance dependence of this process leads to loss of energy transfer by ~15Å, which is consistent with Dexter exchange transfer. Action spectra were acquired and fit to reveal distance constraints for the gas phase structure of the Trpcage in the +2 charge state. In combination with molecular dynamics calculations, it is demonstrated that the data is consistent with retention of the native structure for the +2 charge state.

2.2 Experimental

Peptides

The peptides Ac-RRWWCR-NH_3, CGYGPKKKRKVGG, PHCKRM, VTCG, RGDC, EAGDDIVPCSMSYTWTGK, CQDSETRTFY, and VCYDKSFPISHVR were purchased from American Peptide Company. A series of nine polyalanine helical peptides with sequences Ac-WAAAAAAAACK, Ac-AWAAAAAAACK, Ac-AAWAAAAAACK, Ac-

AAAWAAAAACK, Ac-AAAAWAAAACK, Ac-AAAAAWAAACK, Ac-AAAAAAWAACK, Ac-AAAAAAAWACK, and Ac-AAAAAAAAWCK were synthesized. Additionally, the peptides, Ac-AAAAAAAAACK, VYCG, WWCG, and VWCG were also synthesized. All peptides were synthesized according to standard solid phase peptide synthesis procedures.[32] The Trpcage variants C-Trpcage, Trpcage-C, and Trpcage Y3F were also synthesized by solid phase peptide synthesis.

Disulfide formation

5μL of 3mM peptide solution was combined with 1μL of propylmercaptan and 10μL of DMSO. The mixture was heated in a water bath at 37ºC for 12 hours and then lyophilized to remove DMSO. Samples were resuspended in 200μL 50:50:1 water : ACN : TFA. Disulfides between peptides were formed in the same manner using 5μL of a 3mM solution of each peptide.

Synthesis of Indole-3-methanethiol

Gramine, methyl iodide, potassium thioacetate, and potassium carbonate were purchased from Sigma-Aldrich. 1.2 mmol of gramine was reacted with an excess of methyl iodide (5 mmol) in 5 mL of 1:5 methanol:acetonitrile and stirred for 3 hours. The precipitate was collected by vacuum filtration and rinsed with acetone. The resulting solid was then reacted with an excess of potassium thioacetate (3.6 mmol) in a 5 mL 2:2:1 mixture of tetrahydrofuran:acetonitrile:water. The mixture was stirred vigorously for 4 hours. 2 mL of water and chloroform were added and the organic layer was extracted and washed with water. The resulting organic layer was dried by nitrogen. The product was redissolved in methanol (4 mL) and an excess of potassium carbonate was added and the mixture was

stirred vigorously for 2 hours. The final product identity was confirmed by MS/MS. Disulfide modifications of Indole-3-methanethiol and 1H-indole-3-thiol (purchased from Sigma) were performed in the same fashion as peptide modifications.

Molecular modeling

All calculations and molecular modeling were performed in Maestro (Schrodinger Inc., Portland, Oregon) using the OPLS atomic force fields. To estimate disulfide-to-tryptophan distances in peptides, the cysteine and tryptophan sidechains were rotated in sterically-allowed conformations to find the maximum and minimum distances between the disulfide S atoms and tryptophan C4 and C6. MD runs were performed with no solvent at 270K for 10ns with 100ps equilibration time and 1.5ps time-step intervals.

Simulated annealing calculations were performed on the Trpcage variants up to temperatures of 700K or 1000K. Each simulation included 50 cycles, each cycle beginning at 300K, incrementally raising to 400K, 500K, and 700K or 1000K, before lowering to 300K then 200K.

Mass spectrometry disulfide photodissociation experiments

Peptides solutions were sprayed through an ESI source into an LTQ modified with a 266nm Nd:YAG laser (Continuum, Santa Clara, CA) interfaced with the ion trap.[7] UV-photodissociation experiments are performed by isolating the parent ion and exposing it to a single laser pulse in the ion trap prior to scanning out. The yield of disulfide cleavage is calculated by:

$$PD\ yield = \left(\frac{product\ ion\ intensity}{product\ ion\ + precursor\ intensity}\right) * 100$$

For the vast majority of peptides examined, only a single product ion is observed in significant yield.

A second setup utilized an Nd:YAG optical parametric oscillator (OPO) laser (Opotek Inc., Carlsbad, CA) interfaced with an LTQ at the ion trap. Ions are exposed to a single laser pulse per scan. This setup was used to obtain action spectra of ions in the range of 250-300nm. Laser power levels for each wavelength are recorded.

Action spectra are compiled by calculating the PD yield for each wavelength and normalizing them according to differences in the laser power. It should be noted that the laser power of the OPO is genrally ¼ of that of the 266nm laser, and comparing PD yields obtained between the two instruments reflects this.

2.3 Results and Discussion

It has been demonstrated previously that disulfide bonds can be homolytically cleaved very specifically in the gas phase by UV light.[29,33] For example, if two peptides connected by a disulfide bond are irradiated by 266nm light, only the disulfide bond will be broken and two radical peptides will be produced. The efficiency of this process can vary substantially as shown in Table 2.1, where several examples of PD yields for disulfide bond cleavage from precursor selected peptide pairs are given. The PD yields range from less than 1% to up to 37%. There are several potential factors that may influence PD yields in these experiments. For example, the peptide structure or charge state could potentially influence photon absorption. Alternatively, the presence of noncovalent interactions between the two peptides might prevent observation of the individual peptide radicals even

if the disulfide bond were cleaved. In addition, it is also possible that native chromophores could enhance dissociation for some peptide pairs via EET.

Close examination of the results in Table 2.1 suggests that some of these factors are likely influencing the observed PD yields. For example, sequences containing chromophoric residues (Trp, Tyr, and Phe) appear to undergo disulfide cleavage more efficiently than peptides that do not. This suggests that EET may occur from native chromophores to the disulfide bond. Another notable trend is that higher charge states tend to have the best PD yields for peptide pairs that are observed in multiple charge states. This is evident in CGYGPKKKRKVGG + CQDSETRTFY where only the highest observable charge state has a PD yield greater than 1%, as shown in Table 1. A likely explanation for this observation is that charge repulsion overcomes any noncovalent interactions that otherwise inhibit dissociation of the peptide pairs. In the absence of Coulombic repulsion, two peptide radicals generated by disulfide bond cleavage can simply recombine[10] to regenerate the disulfide bond if the fragments are temporarily held together by noncovalent interactions.

Table 2.1. PD yields for selected peptide pairs.

Peptides		**PD Yield**	**Charge State**
Ac-RRWWCR-NH3 + EAGDDIVPCSMSYTWTGA		37%	4+
CGYGPKKKRKVGG + VCYDKSFPISHVR		24%	6+
VTCG + Ac-RRWWCR-NH_3		13%	2+
CGYGPKKKRKVGG + CQDSETRTFY		13%	5+
CGYGPKKKRKVGG + CQDSETRTFY		<1%	4+
CGYGPKKKRKVGG + CQDSETRTFY		<1%	3+
CGYGPKKKRKVGG + CQDSETRTFY		<1%	2+
RGDC + VTCG		<1%	1+
RGDC + PHCKRM		<1%	1+

In order to potentially quantify the contribution of EET to disulfide PD yield, it is desirable to avoid complications arising from such noncovalent interactions. This can be accomplished in a straightforward manner by replacing one of the peptides with a small organic molecule that is not likely to form any significant noncovalent bonds. Propyl mercaptan (PM) is a small saturated hydrocarbon that cannot form hydrogen bonds or participate in any other strong intermolecular interactions. PM also readily forms disulfide bonds with peptides containing free cysteine residues. Accordingly, cleaving disulfide bonds formed with PM should give a more accurate reflection of the underlying photochemistry.

Table 2.2 shows the PD yields for various peptides connected to PM via a disulfide bond. The PD yields are very high for peptides which contain chromophores, as was also the case for some peptides in Table 2.1. Additionally, the PD yields for peptides modified with PM

are higher than the PD yields obtained from related peptide-pairs. For example, Ac-RRWWCR-NH_3 has a yield of 53% when modified with PM while the yields obtained when attached to other peptides are only 37% and 13% as seen in Table 2.1. Even peptides that contain no chromophores (such as RGDC or VTCG) give PD yields of 6% and 7% respectively whereas these peptides only have a PD yield of less than 1% if bound to each other by a disulfide bond. All of these results are consistent with the idea that peptide pairs can form strong interfering noncovalent interactions and that PM is not sticky and thus gives more accurate PD yields.

Table 2.2. PD yields for peptides tagged with PM.

Peptide bound to Propyl Mercaptan	**PD Yield**	**Charge State**
VWCG + PM	58%	1+
Ac-RRWWCR-NH_3 + PM	53%	1+
CGYGPKKKRKVGG + PM	24%	3+
CGYGPKKKRKVGG + PM	20%	2+
CGYGPKKKRKVGG + PM	16%	1+
PHCKRM + PM	7%	2+
PHCKRM + PM	9%	1+
VYCG + PM	17%	1+
VTCG + PM	7%	1+
RGDC + PM	6%	1+
AcA_5WA_3CK + PM	72%	1+
AcA_9CK + PM	8%	1+

The results in Table 2.2 reveal a strong correlation between the presence of aromatic residues and high disulfide PD yield. In order to investigate whether disulfide dissociation is truly due to EET, we recorded the action spectra for tryptophan, a PM modified cysteine containing peptide (AcA_9CK-PM), and a peptide which contains both cysteine and

tryptophan (AcA_5WA_3CK-PM). The results are shown in Figure 2.1. The AcA_9CK-PM spectrum is characterized by weak absorption and featureless decay in the region from 250-300nm. The tryptophan spectrum shows broad absorption with a single peak at 287nm. This spectrum is consistent with previously reported spectra for tryptophan in the gas phase.[34] The peptide which contains both moieties yields a spectrum that closely resembles the tryptophan spectrum, although it is red-shifted by ~10nm. This spectrum was obtained solely by monitoring homolytic fragmentation of the disulfide bond, which is by far the most dominant fragment observed at all wavelengths. The resemblance of the AcA_4WA_3CK-PM spectrum to the spectrum for tryptophan itself and the observed red-shift both are both consistent with fragmentation that occurs following EET.

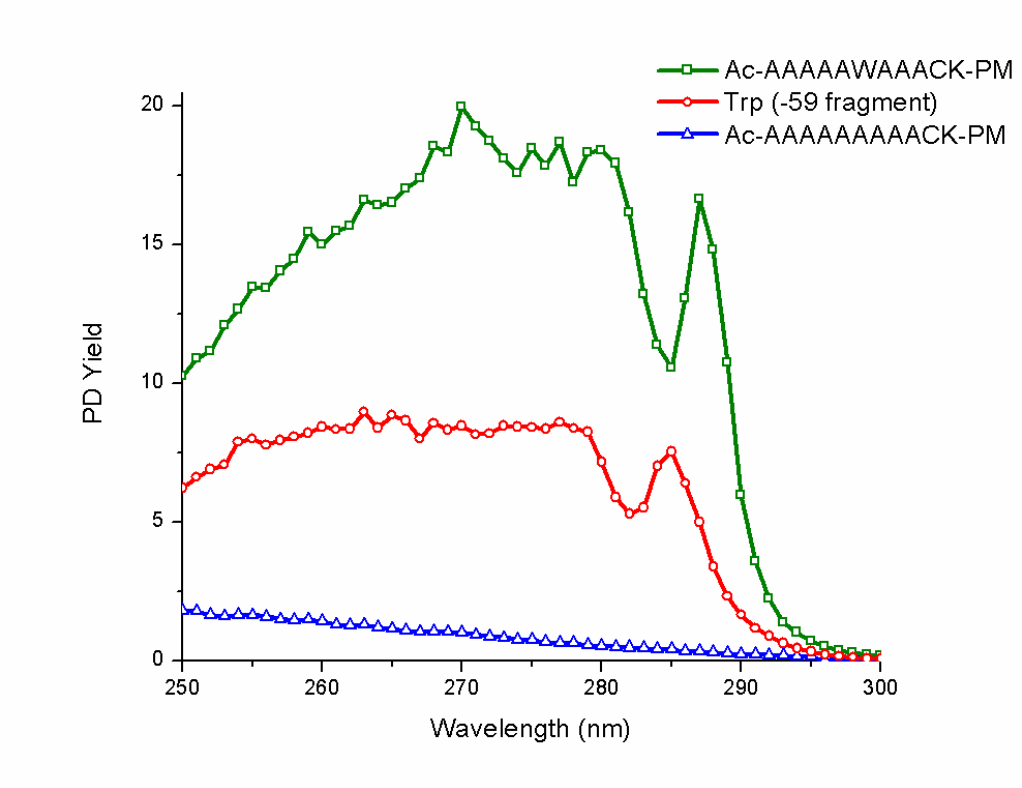

Figure 2.1. Action spectra for AcA_5WA_3CK-PM, tryptophan, and AcA_9CK-PM. Note: PD yields here reflect the lower power of the OPO laser setup and are approximately ¼ of the PD yields reported with the 266nm Nd:YAG.

The results in Figure 2.1 unambiguously establish that PD of the disulfide bond is occurring after excitation of the tryptophan chromophore. In order to determine whether this fragmentation occurs due to EET to a dissociative excited state, we compared the PD spectrum for AcA_5WA_3CK-PM to that obtained by typical collision induced dissociation (CID) and the results are shown in Figure 2.2. The PD spectrum confirms that homolytic fragmentation of the disulfide bond yields by far the most abundant product ion, which is consistent with direct dissociation in the excited state. In contrast, more typical results

consisting of a variety of b and y ions are observed by CID. Importantly, CID in an ion trap strongly favors fragmentation via the lowest energy dissociation pathways. It is clear in Figure 2.2b that homolytic cleavage of the disulfide bond does not occur via a low energy dissociation pathway and is not favored following vibrational excitation. Taken together, the results in Figures 2.1 and 2.2 indicate that the dominant cleavage of the disulfide bond following photoactivation most likely occurs due to excitation of a dissociative excited state. To the best of our knowledge this is the first clear example of a new type of action spectroscopy, where excitation of a donor is followed by energy transfer to a dissociative excited state in the acceptor, leading to bond-specific fragmentation. Importantly, this type of chemistry should also exhibit a distance dependence related to the underlying mode of EET.

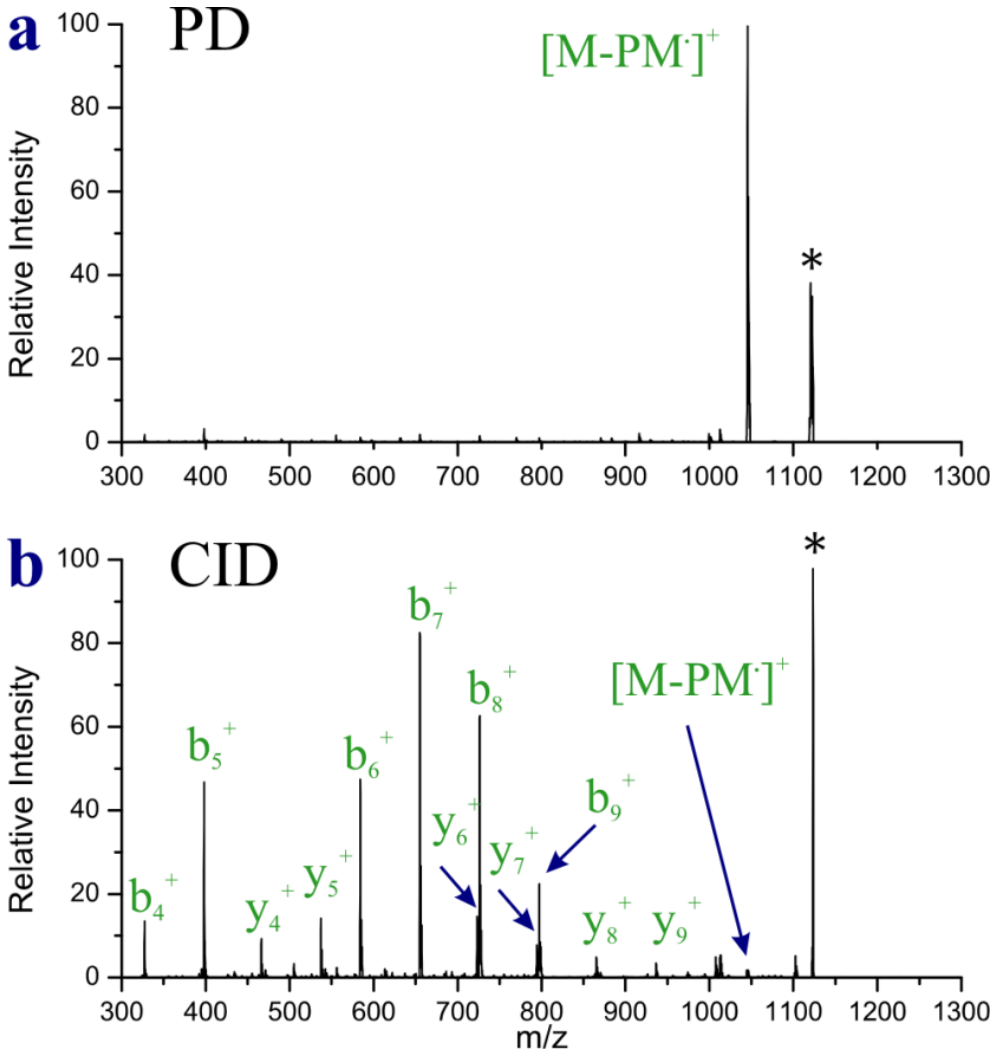

Figure 2.2 (a) PD and (b) CID spectra for Ac-AAAAAWAAACK-PM.

In order to evaluate the distance dependence for Trp/PM EET, we sought to measure the disulfide PD yield for peptides where the distances between donor and acceptor could be reasonably estimated. Previous work has indicated that peptides based on an Ac-A_xK (where $x \geq 7$) motif tend to form alpha helices in the gas phase.[35, 36] Building on this general motif, we synthesized Ac-WA_8CK, which has two of the alanine residues at opposite ends of the helix replaced with PM modified cysteine and tryptophan. The collision cross section for this peptide as determined by ion mobility is consistent with an alpha helical structure

(the predicted cross section of 383.1 Å^2 from molecular modeling matches the experimental data, 372.8 Å^2, within ~3%).The estimated distance between the donor and acceptor for this peptide is ~14.5 ± 2.5 Å. The large uncertainty in the distance comes from the flexibility of the side chains, which are assumed to retain significant rotational freedom. The PD yield for Ac-WA$_8$CK is fairly low at 24%. Nevertheless, the PD yield is still appreciably greater than the 8% obtained for Ac-A$_9$CK, which contains no tryptophan. The results from Ac-A$_9$CK serve as the baseline for inherent non-EET assisted disulfide bond fragmentation in a polyalanine based peptide. It is clear that even at a distance of ~14.5 Å, some EET is occurring.

We also attempted to use the polyalanine scaffold to determine the close contact EET efficiency; however, as the distance between donor and acceptor is decreased by altering donor/acceptor positions in the polyalanine chain, the rotational freedom of the side chains becomes increasingly problematic. Furthermore, it is not clear that peptides where tryptophan replaces a central alanine are able to retain entirely helical structures (i.e. cross sections from ion mobility exceeded 3% difference relative to predicted values). Therefore, we adopted an alternative approach where we simply attached the donor and acceptor to each other via short covalent bonds. Direct attachment of the disulfide bond to the indole chromophore is possible and represents the closest distance that the two moieties can be brought together. By attachment of an amine group on the other side of the disulfide (see structure in Figure 2.4a), a suitable ion can be generated for examination by ESI.

The PD spectrum for the protonated molecule is shown in Figure 2.4a and it contains several interesting features. The expected product at 77 Da results from homolytic cleavage

of the disulfide bond. The intensity of this peak is lower than might be anticipated, given the unavoidable proximity of the donor and acceptor. In addition, several unexpected fragments are observed. For example, there is a peak at 148 Da that corresponds to the radical cation of the indole chromophore. This peak is most likely generated by dissociative electron transfer from the indole ring to the disulfide bond. Indeed, the action spectra for homolytic cleavage of the disulfide bond and electron transfer to the indole are distinct (see Figure 2.3), suggesting formation via distinct chemical processes. No similar signs of electron transfer chemistry were detected in any experiments with peptides. The remaining smaller peaks likely derive from internal conversion of the photon energy to vibrational excitation as the peaks at 108, 118 and 180 Da are also observed by CID (Figure 3b). Other peaks such as 104 and 121 Da may be the result of vibrational excitation of the electron transfer products or some such combination of dissociation pathways.

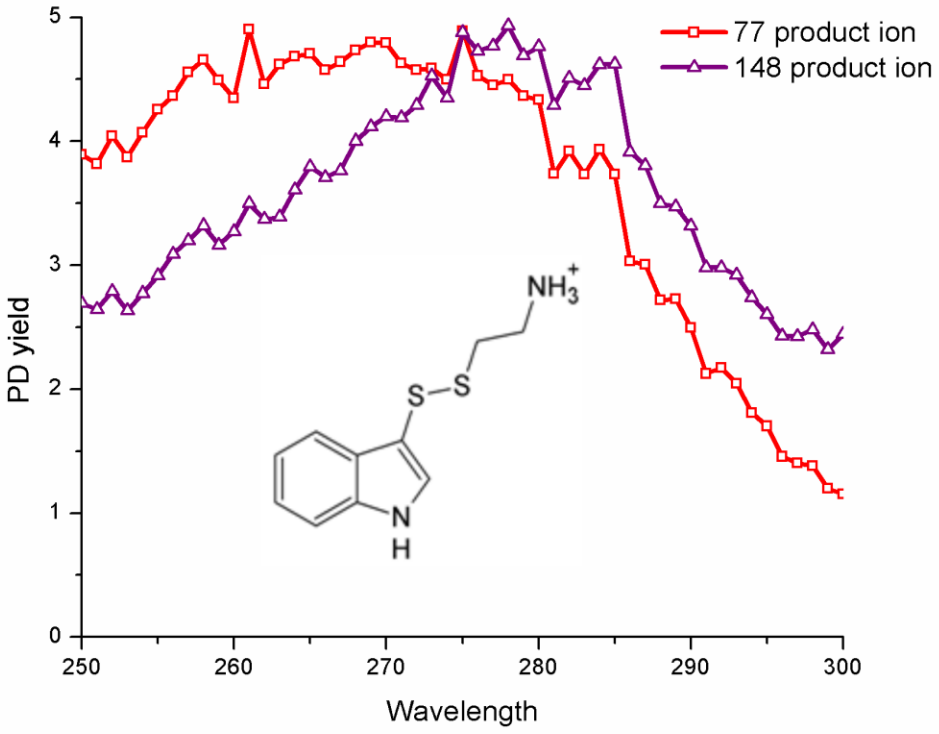

Figure 2.3. Action spectra of both the EET product (77Da) and electron transfer product (148Da) from the dissociation of the pictured structure.

The extremely close proximity of the protonated amine appears to significantly influence the fragmentation behavior of this small molecule. In order to explore this possibility further, we solvated the ammonium group by noncovalent complexation with 18-crown-6 ether (18C6), which forms three strong hydrogen bonds with protonated primary amines.[37] The PD spectrum for the 18C6 complex is shown in Figure 2.4c. The electron transfer product is no longer observed to any significant extent and most other dissociation channels are suppressed as well. Homolytic cleavage of the disulfide bond is enhanced significantly and the resulting PD yield is quite high (~93%). The distance between chromophore centers for the donor and acceptor in this system is ~4 Å, and the

PD yield is likely the maximum value that can be obtained for the indole/disulfide donor/acceptor pair. Insertion of an additional CH_2 group in between the chromophores results in reduced PD yield (88%), consistent with this idea.

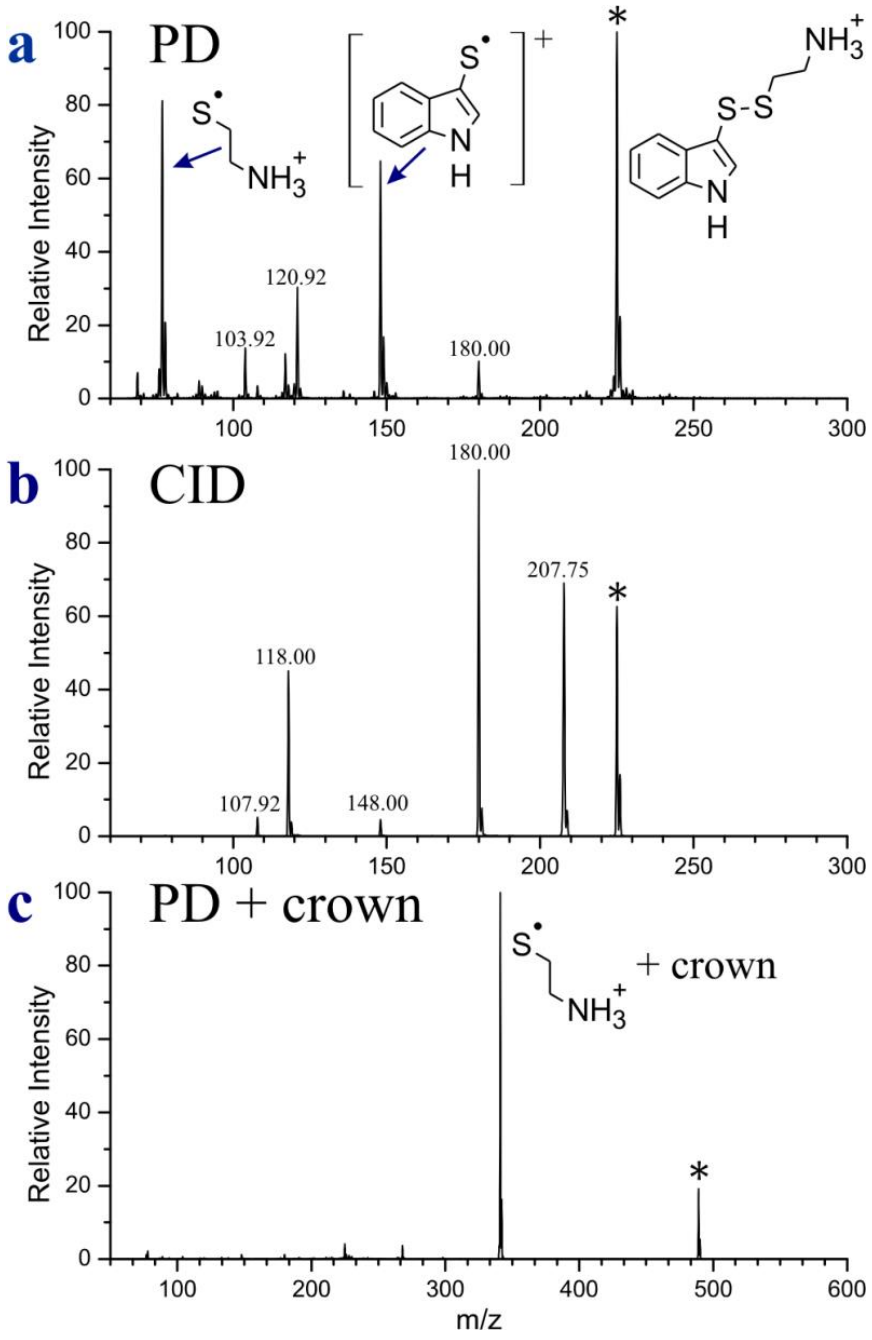

Figure 2.4. (a) PD of the molecule shown to the far right. Structures corresponding to the products of interest are also shown. (b) CID of the same molecule. (c) PD of the same molecule in complex with 18-crown-6.

Given the distance constraints that we have established up to this point, it is possible to narrow down the mode by which EET is likely occurring for this system. The observation that the PD yield decays significantly within 15 Å suggests that FRET is not responsible for most of the energy transfer. Instead, we propose that the indole/disulfide EET occurs primarily via Dexter exchange transfer (DET), which has an exponential distance dependence and typically occurs within 15 Å (Figure 2.5).

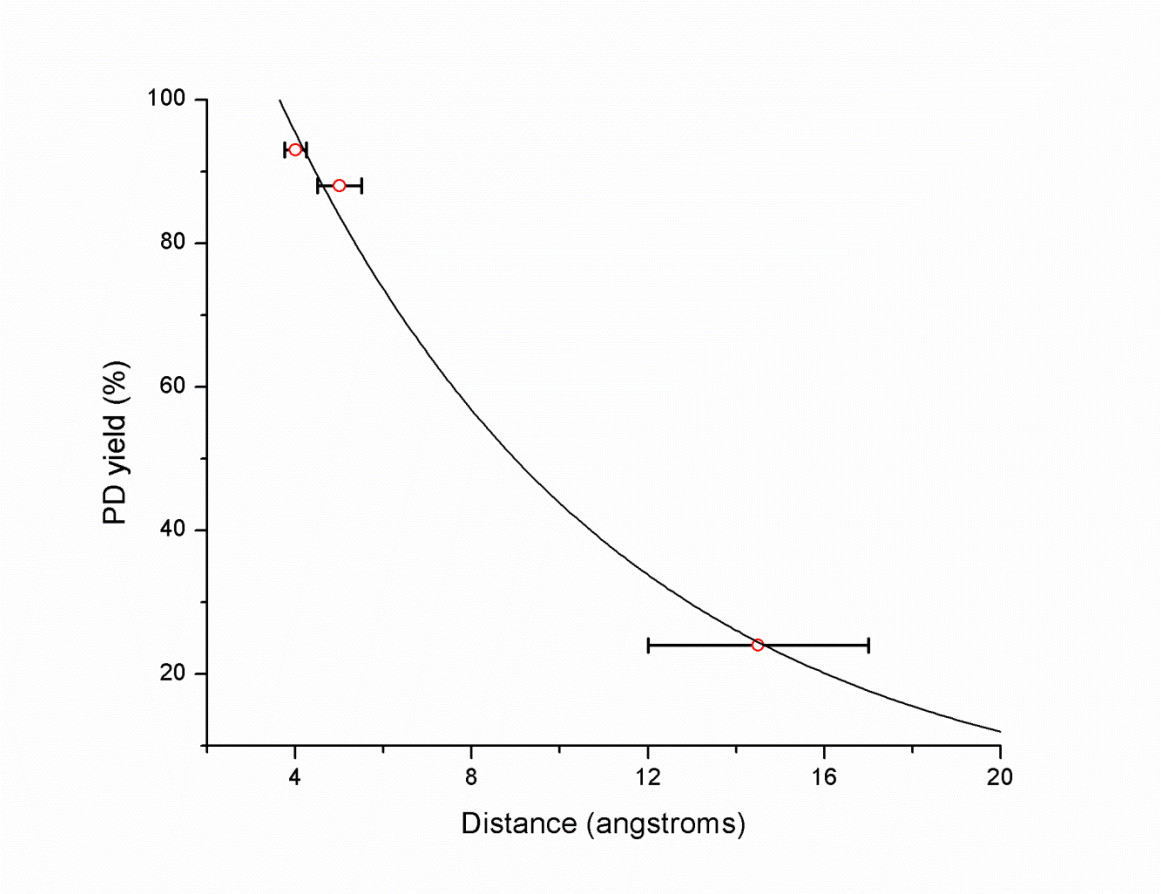

Figure 2.5. Fit of the Dexter equation to the experimental data.

In proteins, Trp is not the only chromophore that may contribute to the cleavage of disulfide bonds via EET. Tyrosine also has significant absorption in the near UV, and would

be expected to facilitate EET mediated disulfide bond cleavage. To explore this possibility further, we replaced tryptophan with tyrosine to create the peptide Ac-A_5YA_3CK-PM, which can be compared with the Trp analog from Figure 2.2. The results are shown in Figure 2.6. The comparison reveals that tyrosine yields a distinct spectrum, which is similar to action spectra acquired for tyrosine itself. The distinctive shoulder occurs at a unique wavelength for both Trp and Tyr, which should allow for contributions from the two chromophores to be distinguished. Furthermore, the Tyr spectrum loses intensity at shorter wavelength more rapidly than Trp. The relative intensity of the Tyr spectrum is also significantly smaller than that for Trp, suggesting that Tyr will only make significant contributions to PD yield at very short distances.

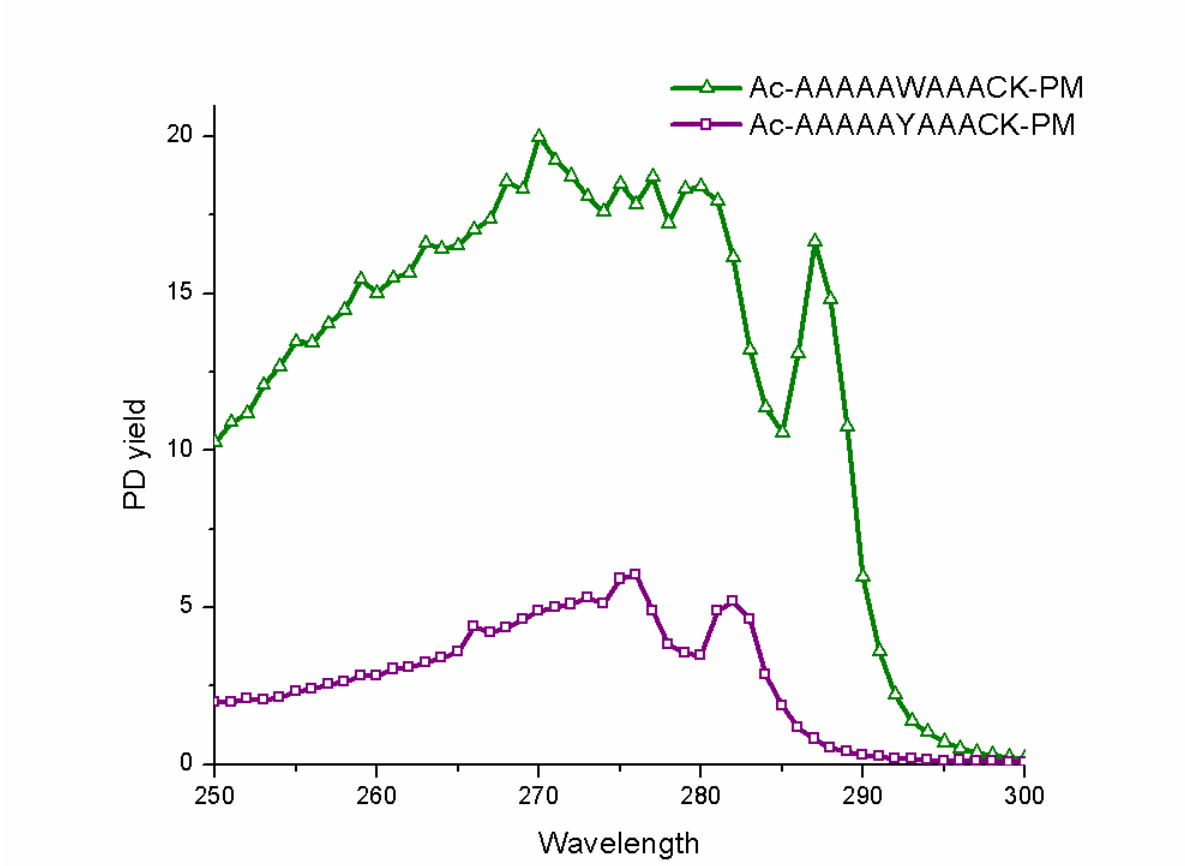

Figure 2.6. Action spectra of Ac-A5WA3CK-PM as compared to Ac-A5YA3CK-PM

Trpcage

We now apply these tools to the examination of protein structure. The Trpcage is a very small and fast folding protein that was designed computationally.[38] It is comprised of only twenty amino acids with the sequence NLYIQWLKDG GPSSGRPPPS. It contains one Tyr and one Trp. The native fold traps the Trp side chain in the center of a hydrophobic pocket created by a small alpha helix and a run of proline residues; this pocket is the defining feature of the structure and the source of the molecule's name. A +−+ salt bridge can form between the Lys, Asp, and Arg side chains. This salt bridge has been demonstrated to be

important for the stability of the protein in solution.[39, 40] An additional salt bridge can form between the N- and C-termini. The stability and importance of these salt bridges in the gas phase has been questioned.[41] Furthermore, previous work has demonstrated that Trpcage can adopt non-native structures in the gas phase.[18] This is not surprising because the gas phase is a very different environment than aqueous solution for which the protein was engineered. Nevertheless, other studies have suggested that native-like Trpcage structures can be stable in the gas phase under appropriate conditions.[42,43]

There are no cysteine residues in the standard Trpcage, therefore, we added a cysteine to both the N-terminus and C-terminus (called C-trpcage and trpcage-C, respectively). NMR experiments reveal that the N and C-terminal residues are fairly disordered, which suggests these additions are not in sterically confined locations and are not anticipated to significantly impact the structure or folding of the protein in solution.

Examination of the action spectra for each charge state, which are shown in Figure 2.7, reveals several important structural features. C-trpcage-PM 2+ exhibits the largest PD yield and the shape of the spectrum is noticeably different from the spectra for other charge states. Importantly, the intensity for this spectrum decreases more rapidly at shorter wavelengths, which is characteristic of EET from tyrosine and indicates very close Tyr/disulfide proximity. At the same time, the shoulder at ~287 nm is indicative of EET from Trp, suggesting that both chromophores contribute to the spectrum. In order to explore this idea further, a combination spectrum created by additively combining the Tyr and Trp spectra is shown in Figure 2.7b. The tyrosine spectrum from Ac-A5YA3CK-PM was combined in a 1:1 ratio with the spectrum from Ac-WA8CK-PM. This would correspond

to a situation where the tyrosine residue is close <6 Å, and the tryptophan residue is significantly farther away (>10 Å). As can be seen in Figure 2.7b, the combination spectrum is a reasonably good match to the experimental C-trpcage-PM 2+ spectrum. The primary differences are due to less distinct absorption at ~282 and ~287 nm, which may be caused by internal solvation of the chromophores. Solvation of tyrosine has previously been demonstrated to yield less distinct spectral features.[44] Alternate ratios of 2:1 or 1:2 mixtures of the same spectra yielded less satisfactory fits.

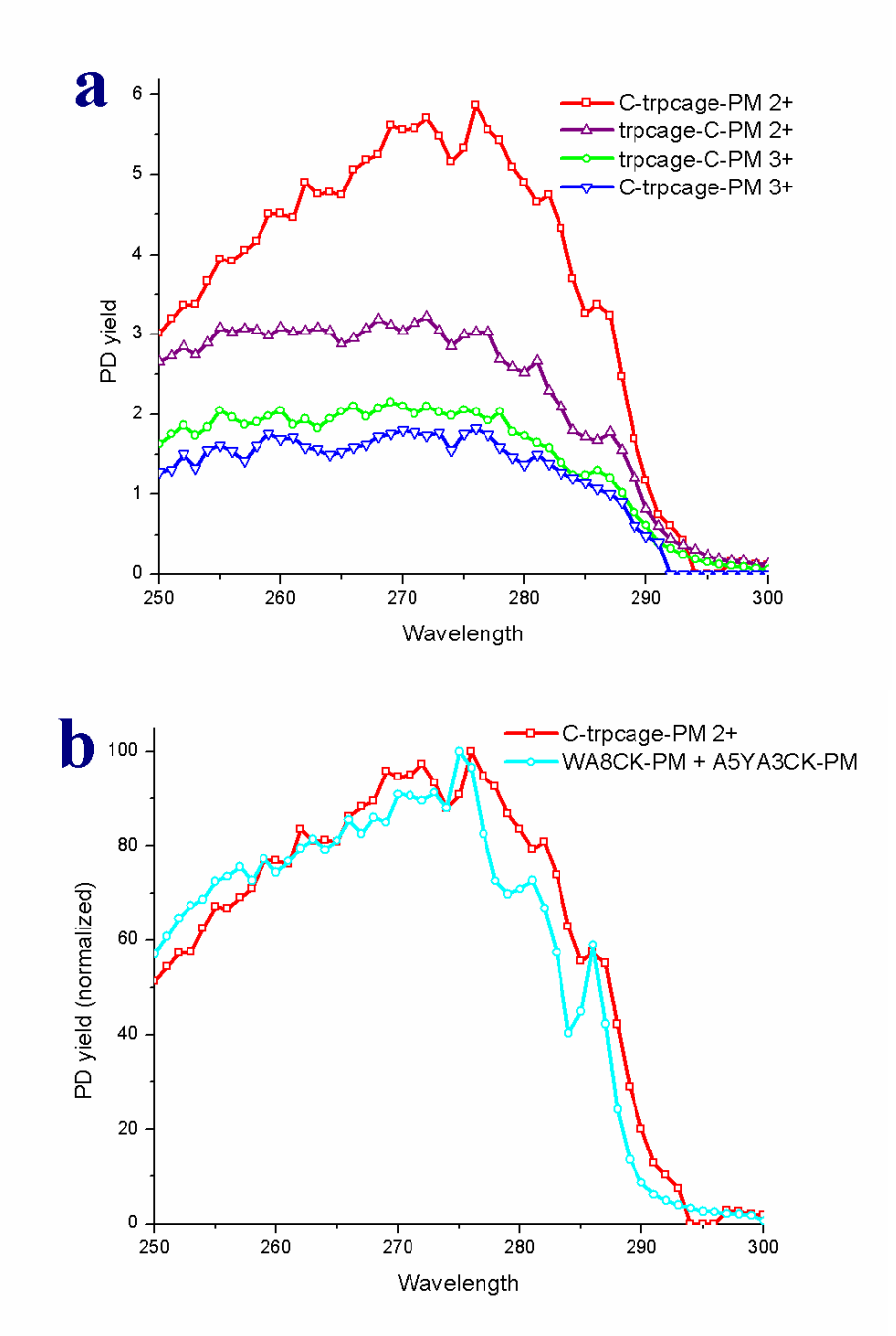

Figure 2.7. a) Action spectra for the C-trpcage 2+, trpcage-C 2+ and trpcage-C 3+. b) Comparison of the action spectrum of the C-trpcage (2+) and the combination spectrum from Ac-A5YA3CK-PM and Ac-WA8CK-PM.

The remaining spectra in Figure 2.7a are significantly flatter and consistent with minimal tyrosine character. To test this hypothesis, a variant of trpcage-C was synthesized with phenylalanine substituted for tyrosine. While phenylalanine is also a potential chromophore, the observed absorption in the 250-300nm range is so poor that we do not detect any appreciable dissociation of phenylalanine containing peptides. Accordingly, spectra for the Y3F mutant of the Trpcage should reveal exclusively EET due to tryptophan. The results are shown in Figure 2.8 overlaid with the spectra collected from the tyrosine-containing version. Differences in the spectra are minimal which supports the idea that tyrosine is too far from the C-terminal cysteine to contribute substantially to EET.

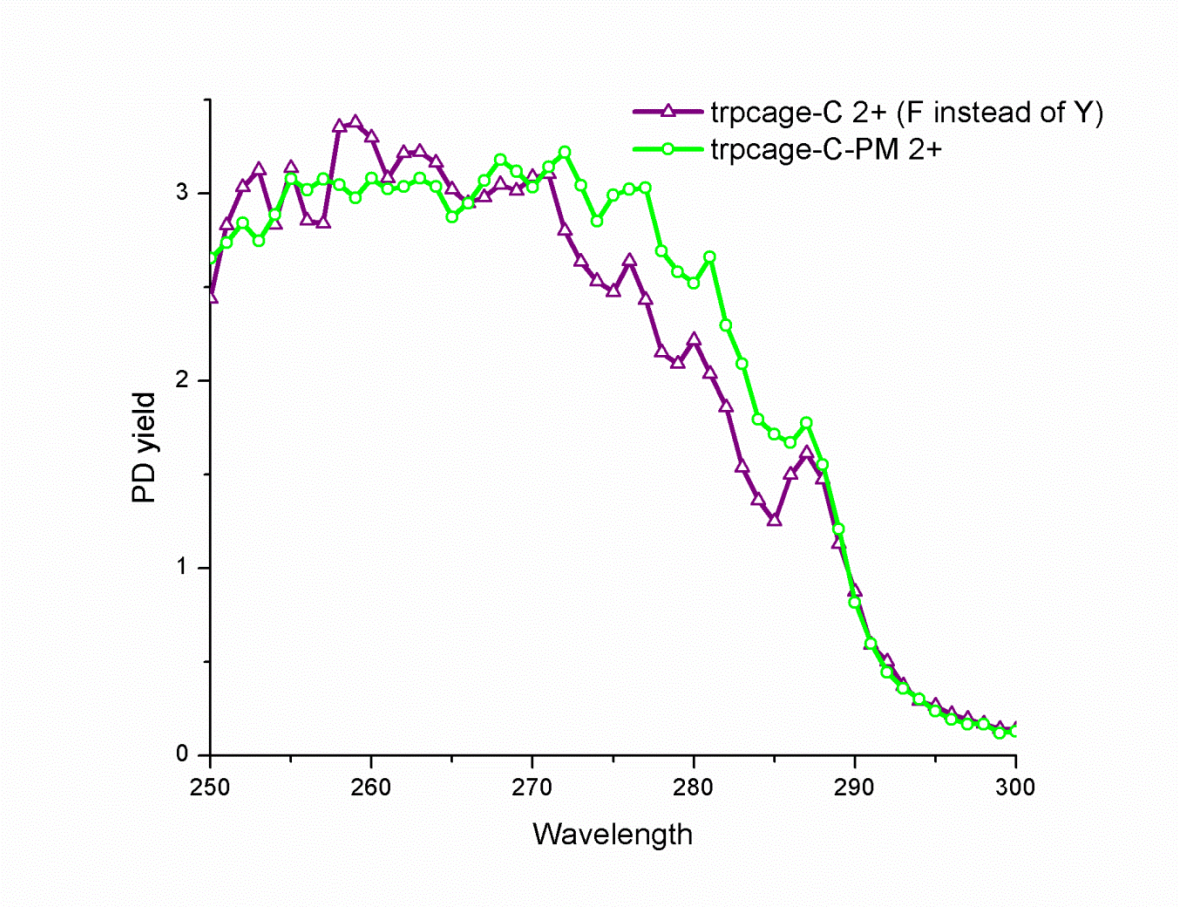

Figure 2.8. Action spectra of trpcage-C-PM and trpcage-C-PM with phenylalanine substituted for tyrosine.

The C-trpcage-PM 2+ is the best candidate for more in depth structural characterization because distance constraint information is provided for both chromophores. Simulated annealing was carried out on the C-trpcage-PM 2+ starting from the native structure. Two separate simulated annealing approaches were used to generate low energy gas-phase structures from the NMR structure: one reaching temperatures of 1000K and another reaching temperatures of 700K. High temperature simulated annealing is preferable to find the global energy minimum, however significant activation to may be required overcome

the energy barriers needed to reach such a structure. Accordingly, the global energy minimum structure generated from simulated annealing at 1000K may not be the structure that is actually observed. In fact, the structure that is generated (Figure 2.9) bears no resemblance to the solution phase structure and is also distinct from those noted in previous studies of the Trpcage.[42,43] In contrast, the structure generated from a more modest 700K annealing resembles the solution-phase structure while being significantly lower in energy than structures generated from other conformational searches or simple energy minimization.

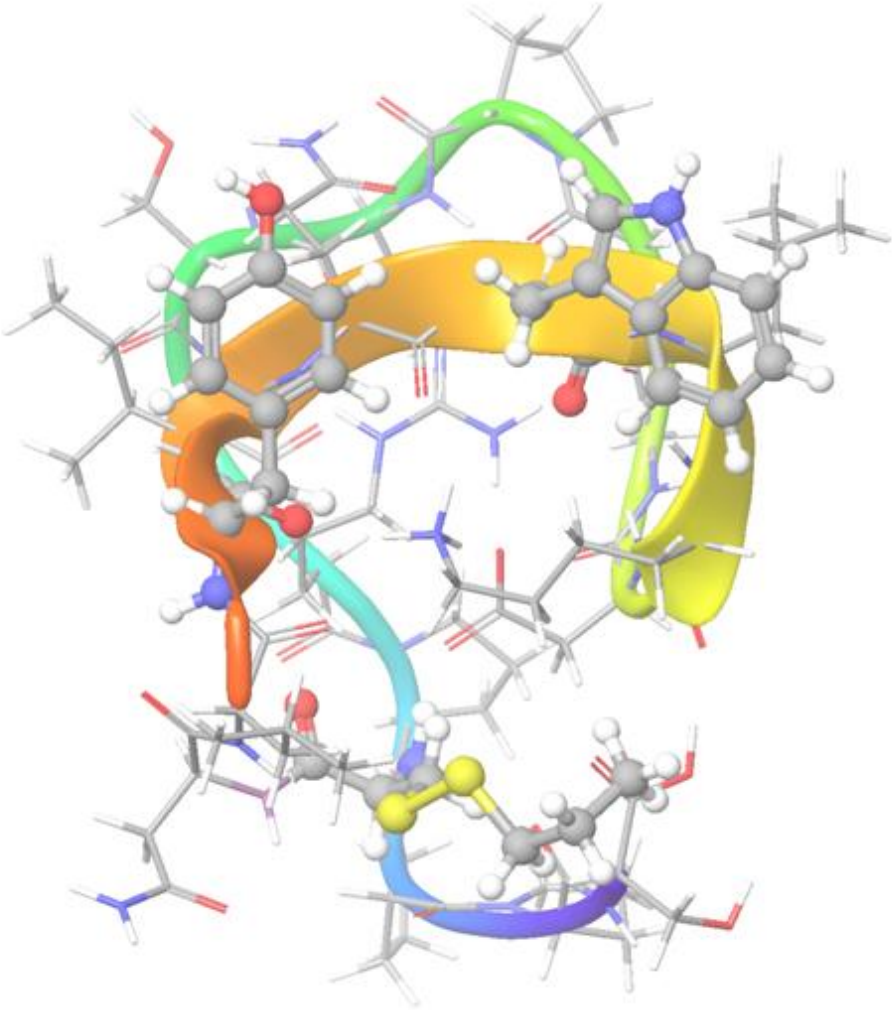

Figure 2.9. Lowest-energy structure generated from simulated annealing at 1000K. Tyrosine, tryptophan and cysteine are represented with ball-and-stick models.

The lowest energy structure obtained from the 700K simulated annealing is shown in Figure 2.10 in comparison with the native structure. Most of the structure is unperturbed, with a few interesting exceptions. Notably, the N-terminus has a different orientation that

allows for extensive hydrogen bonding between the N- and C- termini. The distances between the chromophores and the disulfide bond in the structure in Figure 2.10 are completely consistent with the experimental data in Figure 2.7. It should be noted that one charge is located at the N-terminus, which remains hydrogen bonded to the C-terminus, stabilizing the native-like fold. The second charge is located at arginine, which is in a +–+ salt bridge with Asp and Lys. Previous results have suggested that Trpcage does not retain salt bridges in the gas phase, and that the +2 charge state may not have a native-like structure.[41] There are several possible explanations for these apparent contradictions. The conditions of our source may be gentler, facilitating the retention of the native like structure. It is also possible that the salt bridge may convert to simple hydrogen bond interactions via proton transfer without significantly influencing the remainder of the structure, though previous results with other proteins have demonstrated salt bridges are frequently critical for the retention of native structure in the gas phase.[45, 46] It is also possible that the additional cysteine residue may stabilize the native structure by enabling extra hydrogen bonding between the termini. Comparison of our data with previously proposed structures that differ substantially from the native fold does not yield good agreement (i.e. the Tyr and Trp distances are not consistent with our results). Taking all of the evidence into consideration, we conclude that it is possible to preserve a native like state for the Trpcage in the +2 charge state under appropriately gentle source conditions.

Detailed evaluation of the remaining structures is more difficult, since the data only reveal a fairly long range interaction with Trp and absence of a close range interaction with Tyr. The data for trpcage-C-PM 2+ are consistent with the native fold structure, although

many other structures would likely be suitable as well. Activation of the C-trpcage 2+ structure by harsher source conditions or collisional energy result in significantly lowered PD yields, whereas native MS solvent conditions (1mM NH_4OAc) do not significantly change the yield. This is consistent with the expected unfolding behavior of a native-like structure in the +2 charge state. For the +3 charge states, the results indicate a more unfolded structure, which results in a slightly increased Trp/disulfide interaction distance. This is consistent with previous observations by ion mobility illustrating Coulomb induced unfolding of proteins in higher charge states.[47]

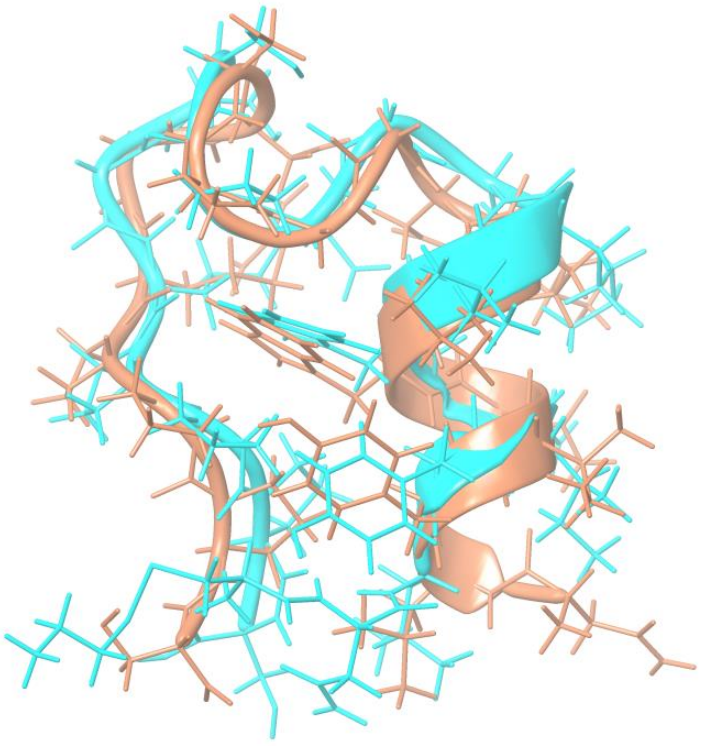

Figure 2.10. Comparison of the C-trpcage-PM simulated annealing structure (blue) superimposed with the Trpcage NMR structure (orange).

2.5 Conclusions

We have developed an action EET system based on Trp/Tyr and disulfide bonds suitable for experiments on ions in the gas phase. Excitation of Trp/Tyr by UV light leads to EET and excited state dissociation of disulfide S-S bonds in a distance dependent fashion. Trp can facilitate homolytic fragmentation of disulfide bonds out to ~15 Å, while Tyr is only active at very close proximity (<6 Å). These distance regimes indicate that the majority of the EET for these chromophores occurs via Dexter exchange transfer and that FRET is likely a minor contributor. The combination of distance information with initiating chromophore identity provides a powerful new platform for investigating protein structure in the gas phase. Furthermore, the ability to use native chromophores (i.e. Trp and Tyr) in combination with disulfide bonds generated from cysteine residues provides facile access to the powerful suite of molecular biology tools that have been developed to manipulate protein sequence. If a native sequence does not contain probes in appropriate locations, standard site-directed mutagenesis can be used to incorporate the desired residues. This presents a considerable advantage over existing methods of applying EET which require more disruptive addition of larger synthetic chromophores. This method should lead to enhancement of our understanding of protein structure in the gas phase.

2.6 Acknowledgements

The authors thank Richard Hooley, Mike Pirrung, and Chris Switzer for helpful advice on synthetic procedures. We thank the NSF for financial support (CHE-0747481) and Greg Beran for stimulating conversation.

2.7 References

[1]M. Yamashita and J. B. Fenn, *J. Phys. Chem.*, 1984, **88**, 4451–4459.
[2]Tanaka, K.; Waki, H.; Ido, Y.; Akita, S.; Yoshida, Y.; Yoshida, T.; Matsuo, T. *Rapid Commun. Mass Spectrom.* 1988, **2**, 151–153.
[3]R. Aebersold and M. Mann, *Nature*, 2003, **422**, 198–207.
[4]E. Jurneczko and P. E. Barran, *Analyst*, 2011, **136**, 20–8.
[5]X. Zhang and R. R. Julian, *Int. J. Mass Spectrom.*, 2011, **308**, 225–231.
[6]J. L. P. Benesch and C. V Robinson, *Nature*, 2009, **462**, 576–7.
[7]T. Ly and R. R. Julian, *J. Am. Chem. Soc.*, 2010, **132**, 8602–9.
[8]S. L. Koeniger and D. E. Clemmer, *J. Am. Soc. Mass Spectrom.*, 2007, **18**, 322–31.
[9]B. C. Bohrer, S. I. Merenbloom, S. L. Koeniger, A. E. Hilderbrand and D. E. Clemmer, *Annu. Rev. Anal. Chem.*, 2008, **1**, 293–327.
[10]X. Zhang and R. R. Julian, *Phys. Chem. Chem. Phys.*, 2012, **14**, 16243–16249.
[11]J. R. Winkler, *Science*, 2013, **339**, 1530–1.
[12]A. Periasamy, *J. Biomed. Opt.*, 2001, **6**, 287–91.
[13]K. Deuschle, *Plant Cell Online*, 2006, **18**, 2314–2325.
[14]R. Roy, S. Hohng and T. Ha, *Nat. Methods*, 2008, **5**, 507–16.
[15]T. Rantanen, M.-L. Järvenpää, J. Vuojola, K. Kuningas and T. Soukka, *Angew. Chemie*, 2008, **120**, 3871–3873.
[16]A. Olaya-Castro and G. D. Scholes, *Int. Rev. Phys. Chem.*, 2011, **30**, 49–77.
[17]A. S. Danell and J. H. Parks, *Int. J. Mass Spectrom.*, 2003, **229**, 35–45.
[18]A. T. Iavarone, A. Patriksson, D. van der Spoel and J. H. Parks, *J. Am. Chem. Soc.*, 2007, **129**, 6726–6735.
[19]A. S. Danell and J. H. Parks, *J. Am. Soc. Mass Spectrom.*, 2003, **14**, 1330–9.
[20]A. T. Iavarone, J. Meinen, S. Schulze and J. H. Parks, *Int. J. Mass Spectrom.*, 2006, **253**, 172–180.
[21]A. T. Iavarone and J. H. Parks, *J. Am. Chem. Soc.*, 2005, **127**, 8606–8607.
[22]M. Dashtiev, V. Azov, V. Frankevich, L. Scharfenberg and R. Zenobi, *J. Am. Soc. Mass Spectrom.*, 2005, **16**, 1481–7.
[23]V. Frankevich, P. Martinez-Lozano Sinues, K. Barylyuk and R. Zenobi, *Anal. Chem.*, 2013, **85**, 39–43.
[24]M. W. Forbes and R. a Jockusch, *J. Am. Soc. Mass Spectrom.*, 2011, **22**, 93–109.
[25]S. K. Sagoo and R. a. Jockusch, *J. Photochem. Photobiol. A Chem.*, 2011, **220**, 173–178.
[26]F. Talbot, A. Rullo, H. Yao and R. A. Jockusch, *J. Am. Chem. Soc.*, 2010, 16156–16164.
[27]R. C. Dunbar, *Int. J. Mass Spectrom.*, 2000, **200**, 571–589.
[28]P. Y. Cheng, D. Zhong and A. H. Zewail, *Chem. Phys. Lett.*, 1995, **237**, 399–405.
[29]C. W. Bookwalter, D. L. Zoller, P. L. Ross and M. V Johnston, *J. Am. Soc. Mass Spectrom.*, 1995, **6**, 872–6.
[30]L.-Z. Wu, Y.-B. Sheng, J.-B. Xie and W. Wang, *J. Mol. Struct.*, 2008, **882**, 101–106.

[31]J. Haywood, O. Mozziconacci, K. M. Allegre, B. A. Kerwin and C. Schöneich, *Mol. Pharm.*, 2013, **10**, 1146–50.
[32] Chan, W. C.; White, P. D. Fmoc Solid Phase Peptide Synthesis, 1st ed.; Oxford University Press: New York, 2000.
[33]A. Agarwal, J. K. Diedrich and R. R. Julian, *Anal. Chem.*, 2011, **83**, 6455–8.
[34]D. Nolting, C. Marian and R. Weinkauf, *Phys. Chem. Chem. Phys.*, 2004, **6**, 2633.
[35]M. Rossi, V. Blum, P. Kupser, G. von Helden, F. Bierau, K. Pagel, G. Meijer and M. Scheffler, *J. Phys. Chem. Lett.*, 2010, **1**, 3465–3470.
[36]R. R. Hudgins, Y. Mao, M. a Ratner and M. F. Jarrold, *Biophys. J.*, 1999, **76**, 1591–7.
[37]R. R. Julian and J. L. Beauchamp, *Int. J. Mass Spectrom.*, 2001, **210-211**, 613–623.
[38]J. W. Neidigh, R. M. Fesinmeyer and N. H. Andersen, *Nat. Struct. Biol.*, 2002, **9**, 425–30.
[39]R. Zhou, *Proc. Natl. Acad. Sci.*, 2003, **100**, 13280–13285.
[40]R. Geney, M. Layten, R. Gomperts, V. Hornak and C. Simmerling, *J. Chem. Theory Comput.*, 2006, **2**, 115–27.
[41]A. Patriksson, C. M. Adams, F. Kjeldsen, R. A. Zubarev and D. van der Spoel, *J. Phys. Chem. B*, 2007, **111**, 13147–50.
[42]C. M. Adams, F. Kjeldsen, A. Patriksson, D. van der Spoel, A. Gräslund, E. Papadopoulos and R. A. Zubarev, *Int. J. Mass Spectrom.*, 2006, **253**, 263–273.
[43]A. Patriksson, E. Marklund and D. van der Spoel, *Biochemistry*, 2007, **46**, 933–45.
[44]B. B. Kirk, A. J. Trevitt, S. J. Blanksby, Y. Tao, B. N. Moore and R. R. Julian, *J. Phys. Chem. A*, 2013, **117**, 1228–32.
[45]X. Zhang and R. R. Julian, *Int. J. Mass Spectrom.*, 2011, **308**, 225–231.
[46]K. Breuker, S. Brüschweiler and M. Tollinger, *Angew. Chemie*, 2011, **123**, 903–907.
[47]D. E. Clemmer and M. F. Jarrold, *J. Mass Spectrom.*, 1997, **32**, 577–592.

Chapter 3: Characterizing gaseous peptide structure with action-EET and simulated annealing

3.1 Introduction

Correctly folded protein structure is essential for biological activity in a vast number of cellular processes. Protein structure and oligomerization also play important roles in various diseases and disorders.[1-3] Accordingly, significant effort has been directed toward using mass spectrometry for structural investigation of proteins. Crosslinking[4], ion mobility[5], non-covalent adduction[6] and radical-based methods[7] serve as a few examples of techniques utilized in this area.

Peptides are smaller subunits of proteins, or in some cases are molecules of biological significance in their own right.[8-11] Peptides are therefore interesting targets of intermediate size, which have received significant attention in gas phase studies.[5,12-21] Ion mobility is the most frequently used gas phase method, where collision cross sections are used in conjunction with theory to evaluate structure. Once a collision cross section has been obtained, ion mobility can provide no further information, which can be problematic for structures that have similar size and energy according to theory.

An alternate method for evaluating peptide structure is to obtain distance constraints between specific parts of the molecule. Crosslinking has been used extensively in solution,[4] and there are also examples in the gas phase.[22,23] Radical

chemistry[24] and energy transfer can also be used to obtain distance constraints.[25-27] In experiments where atom-to-atom distances are revealed, this information can be used to guide calculations toward relevant structural space. This approach has been utilized in cross-linking with great success.[4, 28, 29]

Recently we developed action excitation energy transfer (action-EET), a mass spectrometry-based method that probes the distance between a chromophore and a disulfide bond.[30] Energy transfer is observed by the excited state dissociation of the disulfide resulting in a mass loss (typically propyl mercaptan (PM) radical). Energy transfer happens at distances up to ~15 Å if tryptophan is the chromophore or ~6 Å for tyrosine, giving very tight distance information that is valuable for structural determination. Herein we probe gaseous peptide structure by using action-EET to reveal distance constraints between tyrosine and PM that can guide computational analysis.

3.2 Experimental

Materials

The peptides CDPGYIGSR (laminin B1 fragment), CEGNVRVSRELAGHTGY (GTP binding protein fragment G beta), and YRVRFLAKENVTQDAEDNC (CD36 peptide P 93-110) were purchased from American Peptide Company (Sunnyvale, CA). Propyl mercaptan was purchased from Acros Organics (Geel, Belgium).

Peptide modification

Peptide modification with PM was performed as described previously in [30]. Modified peptide solutions were lyophilized to remove solvent before being re-dissolved in the solvent for analysis.

Action-EET experiments

Action-EET data collection was performed using an LTQ-XL mass spectrometer (Thermo Scientific) coupled with a tunable OPO laser (Opotek Inc., Carlsbad, CA) or an LTQ coupled with a 266 nm Nd:YAG laser (Continuum, Santa Clara, CA) as described in [30]. Modified peptide solutions were sprayed in 10% MeOH in water with 0.1% formic acid. Action spectra were compiled after performing action-EET experiments at varying wavelengths using the OPO laser setup. Photodissociation (PD) yields were obtained by calculating the percent product ion generated in the mass spectrum for a given wavelength. Yields presented in the action-EET spectra y-axis are normalized to the 266 nm dissociation yield (using an Nd:YAG laser) for the given structure, such that PD yields are representative of those obtained with a 4 mJ laser.

Computational simulations

Simulations of peptide structure were performed with the Maestro software suite (Schrödinger Inc., Portland, OR) using the OPLS 2005 atomic force fields. Simulated annealing molecular dynamics were performed as described in [30] up to temperatures of 1000K to yield global energy minimum structures. Simulations were

done with 100 cycles using the beginning at 300 K, incrementally raising to 400, 500, and 1000 K before lowering to 300 K and then 200 K. Constrained simulated annealing was performed in the same manner but with an imposed 4±3 Å distance constraint between two atoms. After constrained simulated annealing, unconstrained energy minimization was performed to test structure stability and give an accurate energy. Semi-empirical calculations were also performed on optimized structures using PM6.[31]

Collisional cross section calculations

Helium collision cross sections were simulated using MOBCAL with the trajectory method.[32]

3.3 Results and Discussion

The Laminin peptide (CDPGYIGSR) action-EET spectra for the 1+ and 2+ charge states are shown in Figure 3.1. The two spectra share similar features including peaks consistent with EET from tyrosine, indicating that the disulfide is within ~6 Å of tyrosine for both structures. Additionally there is information contained within the relative intensities of these spectra. Laminin in the 2+ charge state has a distinctly lower yield than the 1+ charge state. To extract structural information from these spectra, we generated low energy structures for each charge state using simulated annealing molecular dynamics. The lowest energy structures initially obtained for each charge state are shown in Figure 3.2.

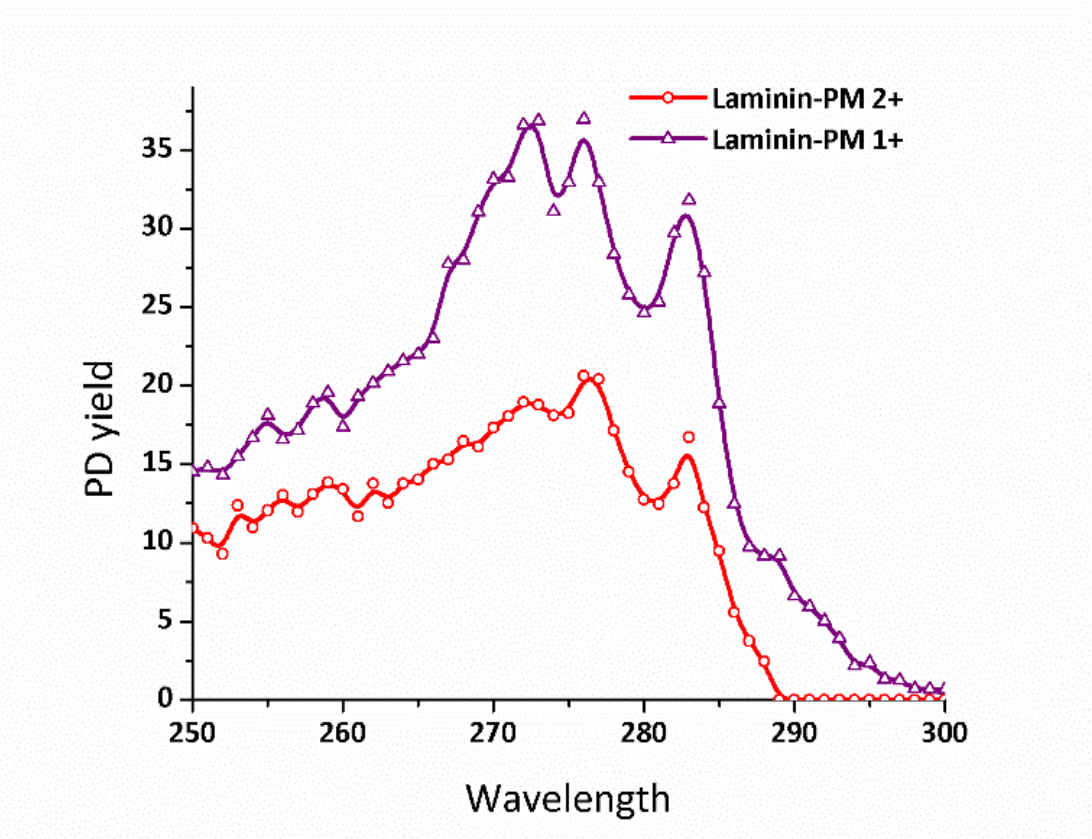

Figure 3.1. Action-EET spectra of Laminin-PM in the 2+ (red) and 1+ (purple) charge states

For the 2+ Laminin peptide (protonation sites will be indicated for each peptide as follows: $N_{term}R_9$, indicating protonation at the N-terminus and Arg9), the lowest energy structure (-1054 kJ/mol) has a disulfide-tyrosine distance of 11.9 Å (Figure 2b). This long distance is inconsistent with the degree of tyrosine mediated EET present in Figure 3.1. Subsequent calculations incorporating a distance constraint between the disulfide and tyrosine (to drive the simulation toward relevant conformational space) were carried out as described in our previous work.[30] The resulting lowest energy structure has a donor-acceptor distance of 4.2 Å (Figure 2c) and is ~5 kJ/mol higher in energy than the original structure, which is within the

uncertainty of this level of theory. For the 1+ charge state ($N_{term}R_9C_{term}$, here indicating that the C-terminus is negatively charged) the lowest energy structure generated by simulated annealing was consistent with the action-EET spectrum, placing the tyrosine and disulfide 5.3 Å apart (Figure 3.2a).

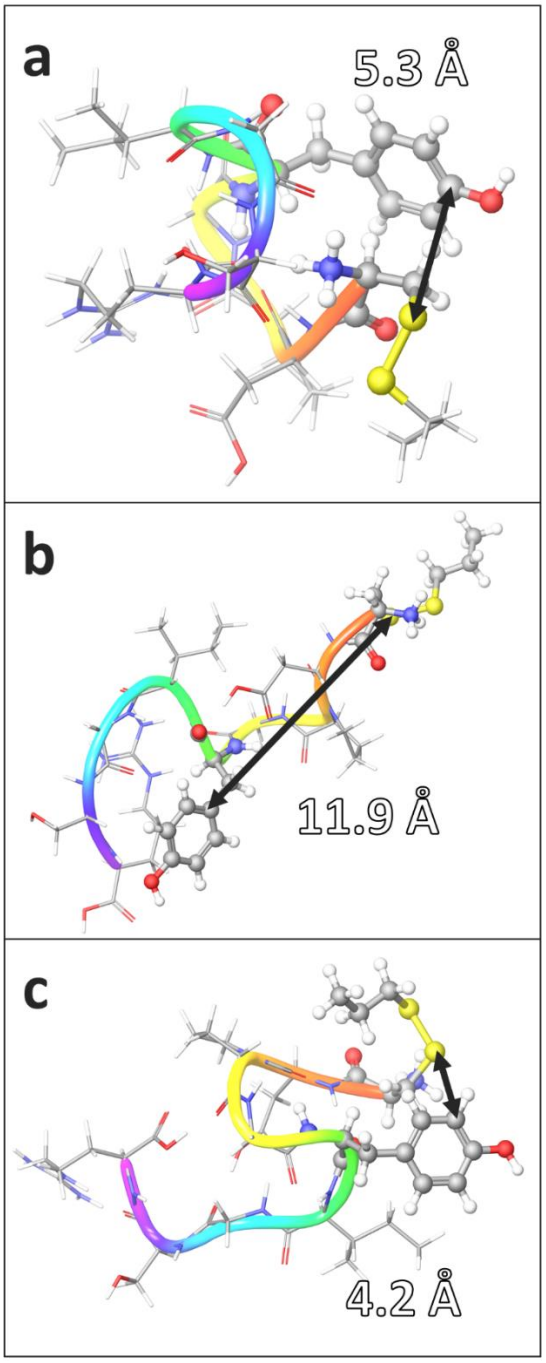

Figure 3.2. structures of Laminin-PM obtained from simulated annealing in the a) 1+ charge state (lowest energy structure) b) 2+ charge state (lowest energy structure) and c) 2+ charge state from constrained simulated annealing. Disulfide-tyrosine distances are shown.

As mentioned above, the relative intensities of the EET spectra for the two charge states are significantly different. There are two possible explanations for this observation. It is possible the Tyr/disulfide distance varies between the two charge states; however, given the tight distance dependence for Tyr→disulfide EET, any gradient in energy transfer should be difficult to observe.[30] Furthermore, the distance in the proposed 2+ structure (4.2 Å) is longer than the 1+ (5.3 Å), suggesting energy transfer should be more prevalent in the 2+ structure. Alternatively, if a heterogeneous population of structures exists for the 2+ peptide where some structures have proximal Tyr/disulfide pairs and others do not, then a reduction in apparent EET would be expected. Indeed this situation is suggested by simulations, which yield two low energy structures fitting these criteria. Semi-empirical calculations for these structures suggest that the two 2+ structures have energies of -1489 (long donor-acceptor distance) and -1536 (short donor-acceptor distance) kJ/mol, putting them within 47kJ/mol of each other in the opposite energetic ordering relative to molecular dynamics. Interestingly, ion mobility collision cross sections for the two structures of the 2+ charge state are 265 and 267 Å, suggesting that ion mobility measurements would not be able to resolve these conformers.

Figure 3.3 shows the action-EET spectra for the GTP-binding fragment peptide (CEGNVRVSRELAGHTGY). The 2+ charge state clearly exhibits tyrosine mediated EET absorption features. The spectrum for the 3+ charge state is quite different and does not illustrate abundant absorption. For the GTP 2+ peptide (R_6R_9), the lowest energy structure (-2560 kJ/mol) obtained by simulated annealing has a

Tyr/disulfide distance of 4.8 Å (Figure 3.5a). This structure is consistent with the action-EET spectrum.

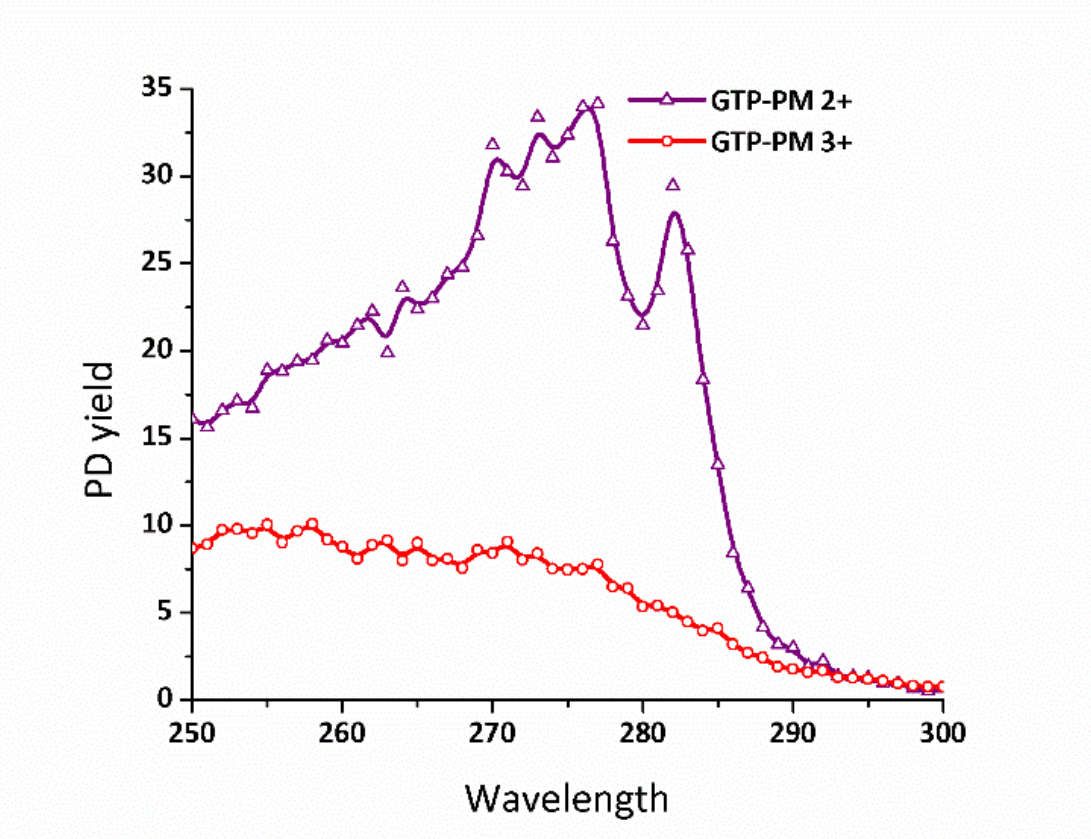

Figure 3.3. Action-EET spectra of GTP-PM in the 2+ and 1+ charge states

For the 3+ peptide, ($R_6R_9H_{14}$) the lowest energy structure (-2275 kJ/mol) puts tyrosine 6.2 Å away from the disulfide (Figure 3.5b). This distance is close to the ~6 Å cut-off distance for tyrosine EET. Closer examination of the 3+ spectrum indicates some additional absorption compared to an isolated disulfide spectrum without any enhancement by EET (see Figure 3.4). This indicates that there may be a small amount of energy transfer from tyrosine for the 3+ peptide. This result is consistent with the results from simulated annealing, where the distance is at the

edge of potential EET. The lack of distinct absorption features in the spectrum is indicative of hydrogen bonding to a charged site, which is also seen between histidine and the tyrosine OH in the annealed structure (Figure 3.5c). Hence the data is consistent with the lowest energy structures for both charge states.

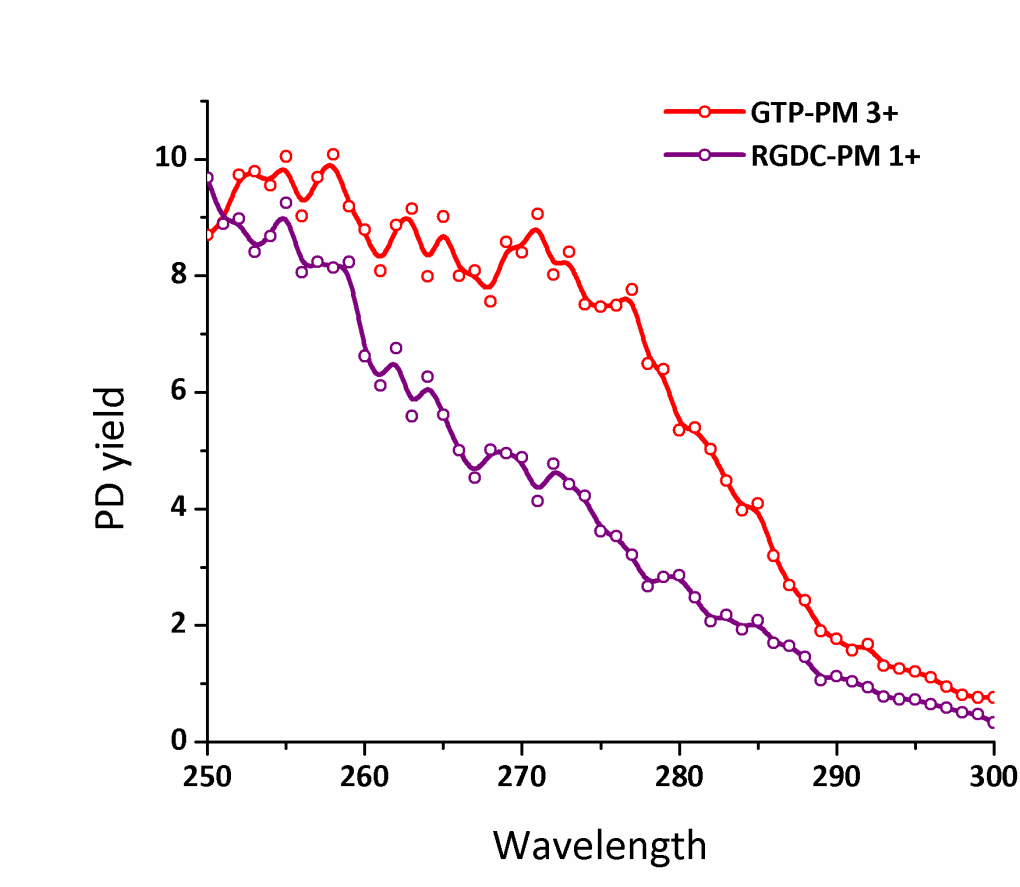

Figure 3.4. Action-EET spectra of GTP-PM 3+ and RGDC-PM 1+ for comparison.

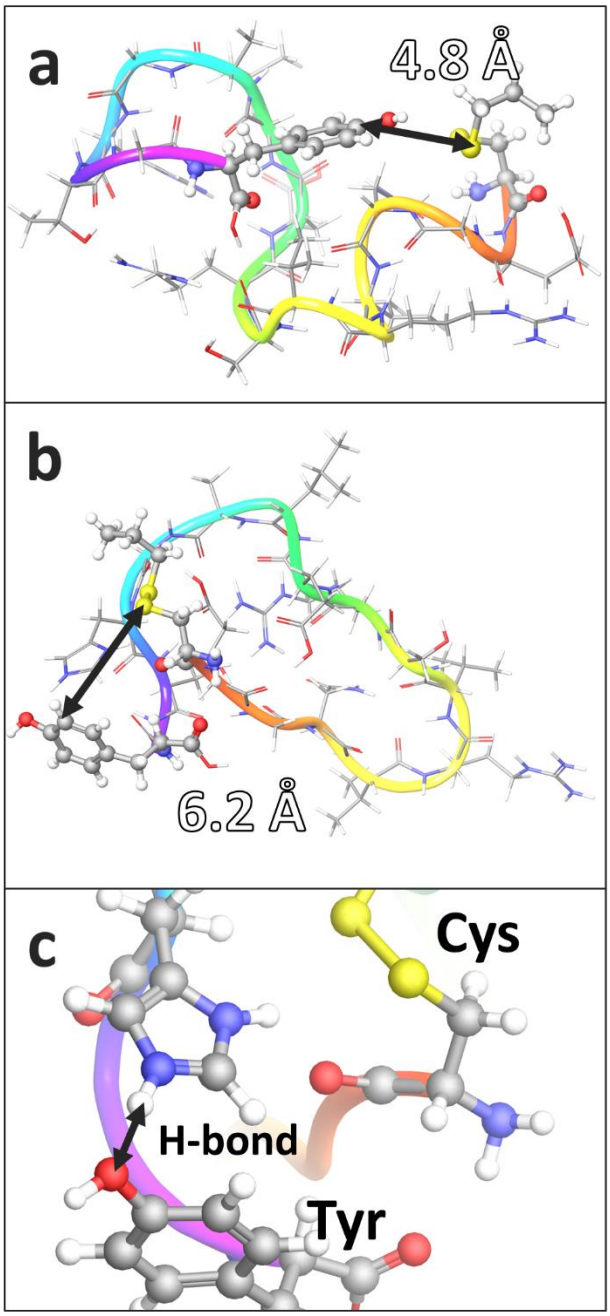

Figure 3.5. structures of GTP-PM obtained from simulated annealing in the a) 2+ charge state (lowest energy structure) b) 3+ charge state (lowest energy structure) and c) a zoom-in of the 3+ structure.

Determining charge configurations for peptides

Next we examine the CD36 93-110 peptide (YRVRFLAKENVTQDAEDNC). Action-EET spectra for this peptide in the 2+ and 3+ charge states are shown in Figure 3.6. There is moderate absorption in the tyrosine EET region for both charge states, indicating proximity between Tyr/disulfide. Additionally, in both spectra the distinct peak at ~285nm is dulled, suggesting hydrogen bonding to the OH group of the tyrosine side chain.[30]

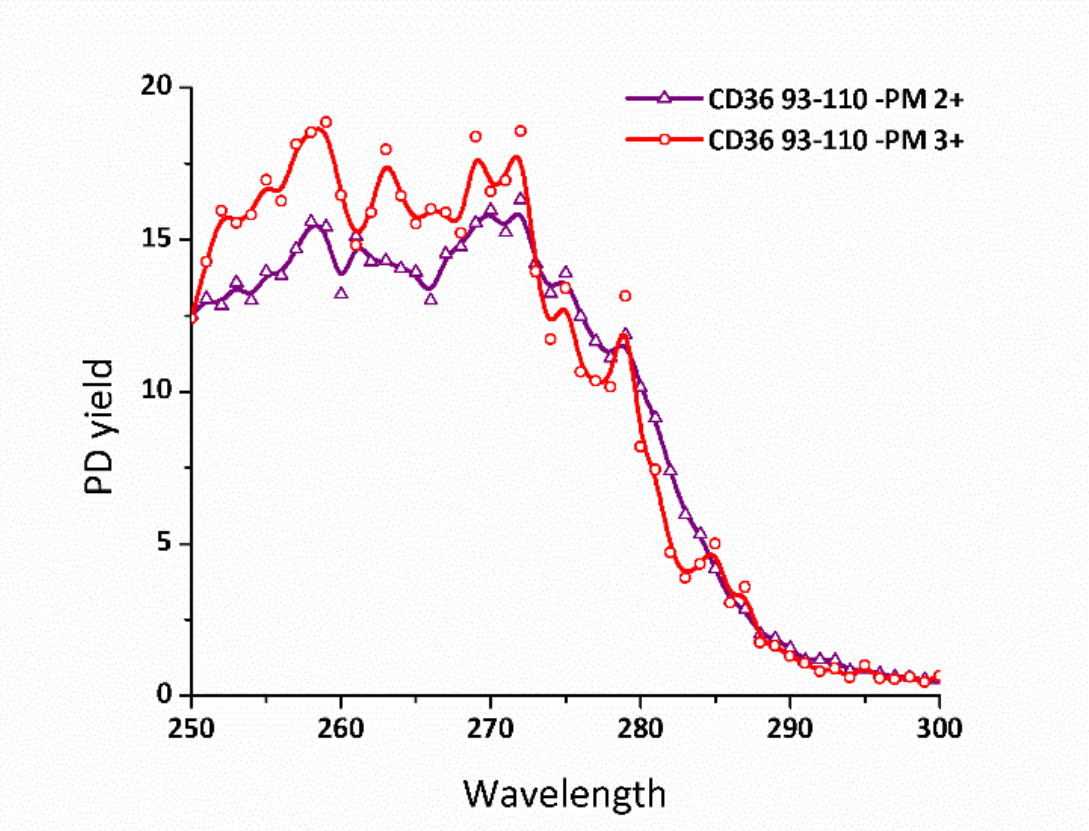

Figure 3.6. Action-EET spectra of CD36 93-100-PM in the 2+ and 3+ charge states

Computational evaluation of this peptide is immediately complicated by the sequence, which contains numerous acidic and basic residues. Thus far, determining where to protonate peptides has either been unambiguous or limited to a few options, allowing for investigation of all possibilities. However many peptides have numerous basic and acidic sites such that charge states can be obtained by various possible protonation/ deprotonation combinations. The CD36 93-110 peptide, for instance, has 5 acidic and 4 basic sites. Accordingly, assigning charges is a non-trivial matter, there are 9 possible configurations for the 3+ ion and 36 possible configurations for the 2+ peptide. Simulated annealing of all these states is not reasonable, so we have developed an alternate approach that leverages the experimentally determined distance constraint.

First, the observed distance constraint is imposed on an entirely neutral peptide, and simulated annealing is used to determine the lowest energy structure. Second, the resulting structure is examined to determine likely positions where charged sites, including salt bridges, could exist without disrupting the structure. In other words, if acidic and basic sites are in close proximity, they will be deprotonated and protonated to investigate if the resulting salt bridge is favorable. For net charges, they are tested at sites that are most basic, and furthest apart from each other. Numerous potential structures can meet these criteria, but far less than would be tested by randomly assigning *every* charge state conformer. Finally, potential structures are examined without distance constraints to identify the lowest energy conformation.

In the neutral structure for CD36 93-110 (Figure 3.7a), Asp15 and Arg4 are connected via strong hydrogen bonds (Figure 3.7b). This interaction can be substituted with a salt bridge, but does not change the net charge of the molecule. An additional site appears to be a likely location for a salt bridge due to proximity of acidic/basic sites (C-terminus/Arg2, Figure 3.7c). A salt bridge between these sites is reasonable because it should bring the two termini close together (which contain the cysteine and tyrosine residues that are experimentally known to be in close proximity).

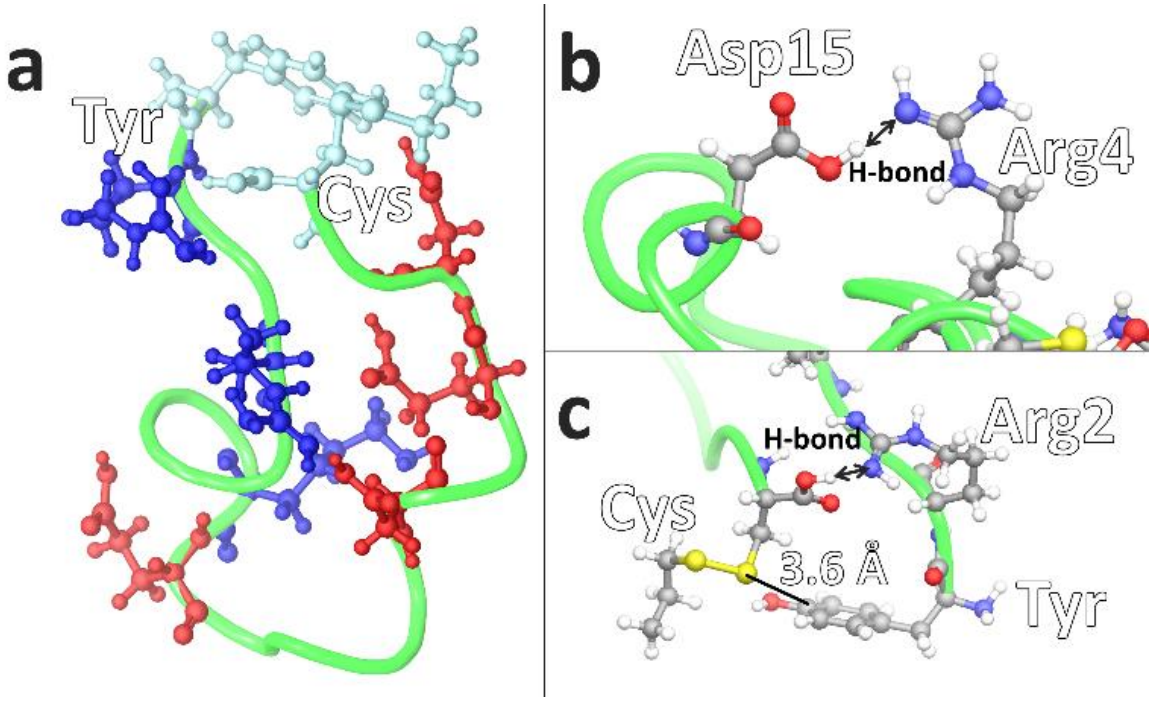

Figure 3.7. Simulated annealing results for the lowest energy structure of the constrained, neutral CD36 93-110-PM peptide (a). Basic residues are shown in blue and acidic residues are shown in red. The Cys and Tyr residues, which are the N- and C-terminal residues respectively, are shown in light blue. Positions where there is hydrogen bonding between acidic and basic sites are shown in (b) and (c).

Using the approach described above, we explored the charge configuration $N_{term}R_2R_4K_8D_{15}C_{term}$ for the 2+ charge state. This configuration of charges enables

formation of both hypothesized salt bridges, and thus the product may have a structure resembling that of the neutral constrained structure in Figure 3.7a. This charge configuration of the peptide was subjected to our normal simulated annealing molecular dynamics approach without constraints. The resulting lowest energy structure (Figure 3.9a) has a disulfide-tyrosine distance of 3.9 Å and energy of -4478 kJ/mol. Thus we were able to obtain a highly consistent, plausible structure for the peptide despite a large number of possible charge configurations that can complicate analysis. For comparison, an alternate charge configuration with one less salt bridge, $R_2R_4K_8C_{term}$, generates a structure where the disulfide-tyrosine distance is 9.7 Å (-3833 kJ/mol, Figure 3.8). This particular charge configuration is also substantially higher in energy than the structure found to be consistent with the experiment.

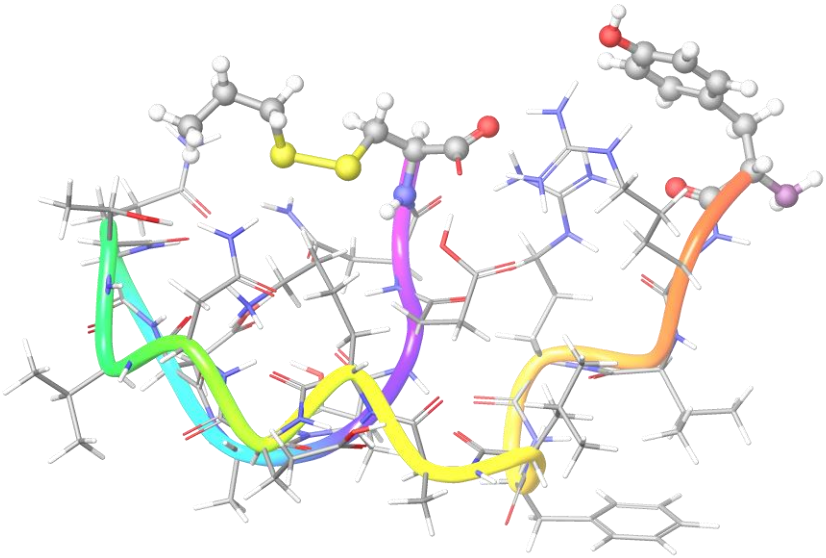

Figure 3.8. CD36 93-110 2+ LES ($R_2R_4K_8C_{term}$)

For the 3+ structure, it is only possible to retain at most one salt bridge while having the desired charge state. By examining the structure in Figure 3.7, the C-terminus/Arg2 salt bridge is important for retaining a structure where the donor and acceptor are near. As noted previously, this particular salt bridge would provide a strong interaction bringing the two terminal regions close together. This configuration could be expected to promote a small donor-acceptor distance since the tyrosine and cysteine are terminal residues. However, the Asp15/Arg4 salt bridge position stabilizes a turn in the backbone that could also perceivably place the terminal regions near each other. Accordingly, both configurations were investigated. The initial unconstrained computation with charge configuration $N_{term}R_2R_4K_8C_{term}$ did not yield a structure consistent with the experiment (-3781 kJ/mol, 9.4 Å), however a second, constrained computation generated a structure that put the donor and acceptor only 3.8 Å apart (Figure 3.9b, -3719 kJ/mol). Semi-empirical energy calculations of these structures showed that the energy difference between these two structures is small: -5130 kJ/mol (lowest energy structure) versus -5107 kJ/mol for the structure consistent with the experimental data. Thus there is no significant energy difference between these structures.

For the $N_{term}R_2R_4K_8D_{15}$ configuration, the lowest energy structure from simulated annealing was not consistent with a small donor-acceptor distance (-3784 kJ/mol, 8.0 Å). After constrained simulated annealing, a structure with energy -3738 kJ/mol and distance 5.2 Å was obtained (see Figure 3.10). Semi-empirical calculations however showed the experimentally consistent structure has an energy of -5122

kJ/mol versus -5127 kJ/mol for the lowest energy structure, again indicating no significant energy difference between the two structures. From the action-EET spectra it is clear that tyrosine is near the disulfide in the actual structure of the peptide. In this case two charge configurations yield similarly consistent structures which are not discernable energetically. It's plausible that a combination of both charge configurations are present for this peptide, however we can rule out other structures based on their long donor-acceptor distance.

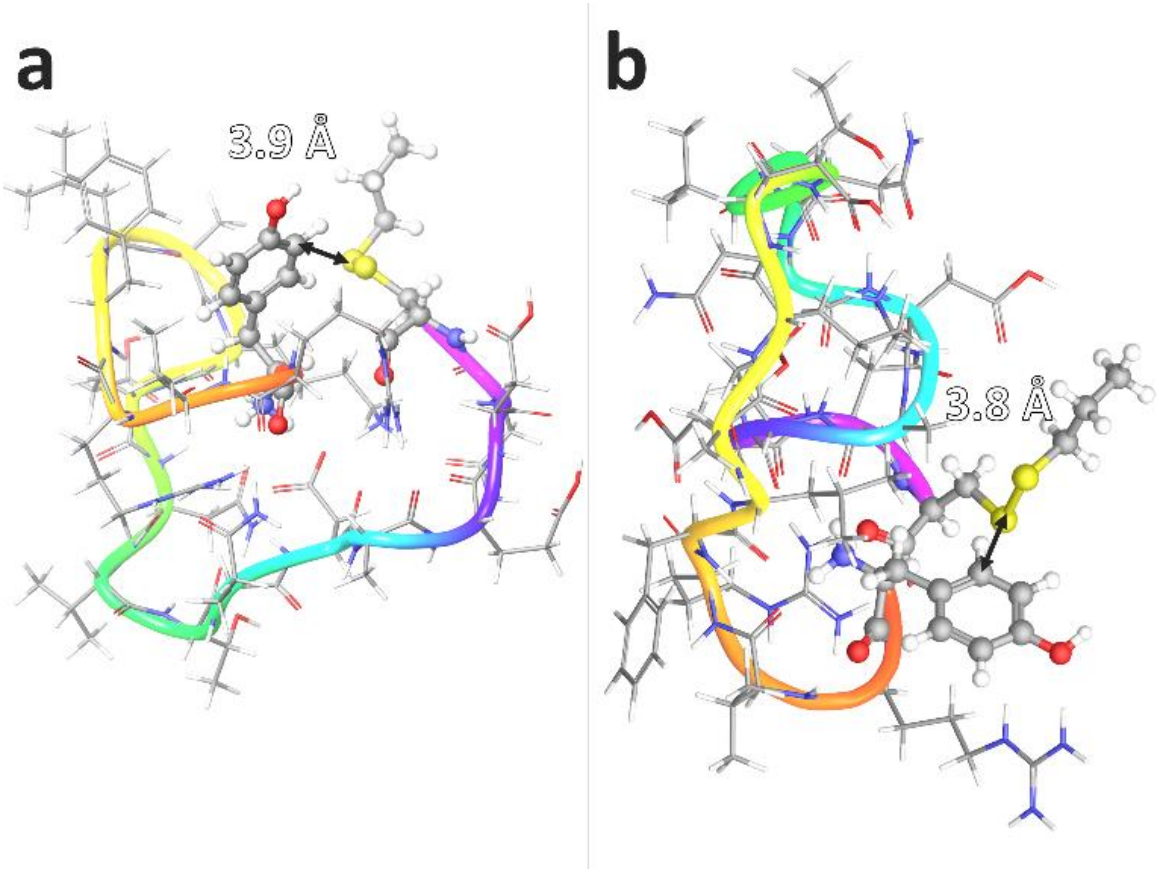

Figure 3.9. Simulated annealing results for the lowest energy structure of the (a) +2 CD36 93-110-PM peptide ($N_{term}R_2R_4K_8D_{15}C_{term}$) and (b) +3 charge state ($N_{term}R_2R_4C_{term}$)

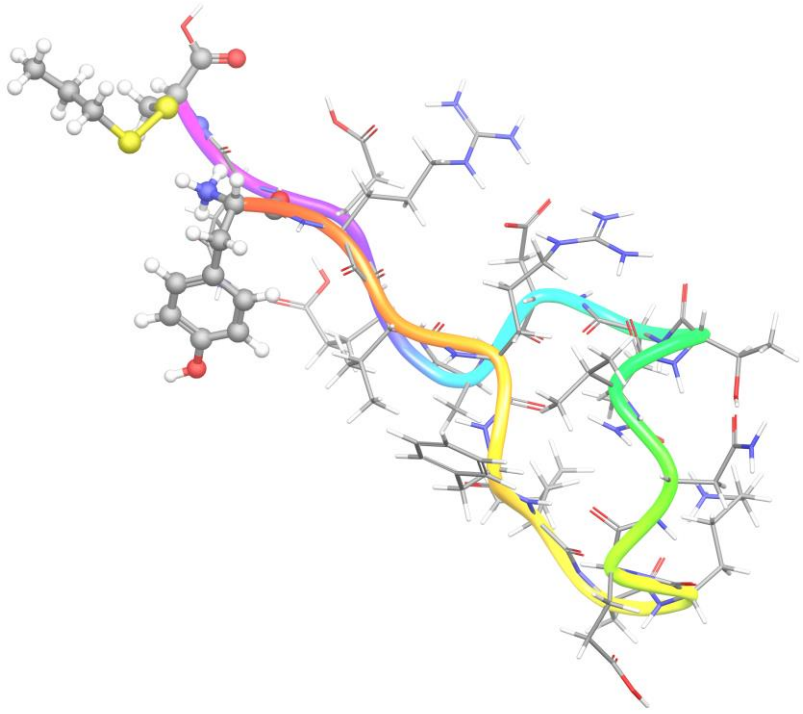

Figure 3.10. CD36 93-110 3+ ($N_{term}R_2R_4K_8D_{15}$) structure from constrained simulated annealing.

Prospects of ion mobility for these structures

Table 3.1 shows the simulated collision cross sections for a selection of low-energy structures for peptides in various charge configurations that are both consistent and inconsistent with the action-EET data. The GTP peptide in the +1 charge state is also included. The calculated CCS values for some of the many possible charge configurations of GTP 1+ highlight how little variance there is for peptide CCS values. For the CD36 93-100 peptide, the lowest energy structure consistent with experimental data ($N_{term}R_2R_4K_8D_{15}C_{term}$) and the alternate charge configuration lowest energy structure that is inconsistent with experimental data

($R_2R_4K_8C_{term}$) have CCSs within <1% of each other. The proposed 3+ ions, on the other hand, do have significantly different CCSs and should be distinguishable by ion mobility. These structures, however, were not suggested by lower-level calculations to be lowest energy conformers. Only after the use of distance constraints and semi-empirical energy calculations did it become evident these were likely structures for the peptide. Laminin 2+ has two structures which are expected to be adopted, but both CCSs are also within <1% of each other and may not be distinguishable as a combination of multiple structures by ion mobility experiments of nominal resolution. Ion mobility, as previously mentioned, is one of the most frequently applied methods for distinguishing protein and peptide structures. While powerful for comparing protein conformations, the small, generally globular structures of peptides do not generally have distinct CCS values, as demonstrated by these calculations.

Table 3.1. Collisional cross sections for various structures and charge configurations of peptides.

Peptide structure and charge configuration	Collisional cross section ($Å^2$)
GTP 1+ $N_{term}E_2R_6R_9E_{10}H_{14}C_{term}$	361
GTP 1+ $E_2R_6R_9E_{10}H_{14}$	368
GTP 1+ R_7	379
GTP 1+ R_{10}	377
CD36 93-110 2+ $N_{term}R_2R_4K_8D_{15}C_{term}$	424
CD36 93-110 2+ $R_2R_4K_8C_{term}$	427
CD36 93-110 3+ $N_{term}R_2R_4K_8C_{term}$	447
CD36 93-110 3+ $N_{term}R_2R_4K_8D_{15}$	384
Laminin 2+ lowest energy structure $N_{term}R_9$ (11.9 Å)	265
Laminin 2+ $N_{term}R_9$ (4.2 Å)	267

3.4 Conclusions

Action-EET provides a wealth of information about the structures of the peptides that would be difficult to obtain with other methods. For example, action-EET

reveals a bimodal distribution of structures for laminin 2+ ions, and the existence of specific intramolecular interactions in the GTP peptide. Determining the convoluted charge configurations for peptides can also be aided through action-EET results, as demonstrated with CD39 93-110. Charge conformer assignment is an obstacle that must be surmounted in order to utilize any computational approach. Action-EET derived distance constraints can further guide simulations towards relevant structures, or be used to rapidly assess the viability of any given structure within a pool of possibilities. Further development of this method will continue to enhance our ability to understand the factors which dictate gaseous structures of complex molecules.

3.5 Acknowledgements.

This work was supported by the National Science Foundation, grant CHE1401737.

3.6 Notes and references

[a] Department of Chemistry, University of California, Riverside, 501 Big Springs Road, Riverside CA 92521

†Data not yet published.

[1] A. Roher, J. Lowenson, S. Clarke, C. Wolkow, R. Wang, R. Cotter, I. Reardon, H. Zurcher-Neely, R. Heinrikson and M. Ball, *J. Biol. Chem.*, 1993, **268**, 3072–3083.
[2] M. D. Kirkitadze, G. Bitan and D. B. Teplow, *J. Neurosci. Res.*, 2002, **69**, 567–577.

[3] K. A. Conway, S. J. Lee, J. C. Rochet, T. T. Ding, R. E. Williamson and P. T. Lansbury, *Proc. Natl. Acad. Sci. U. S. A.*, 2000, **97**, 571–6.
[4] A. Sinz, *Mass Spectrom. Rev.*, 2006, **25**, 663–82.
[5]B. C. Bohrer, S. I. Merenbloom, S. L. Koeniger, A. E. Hilderbrand and D. E. Clemmer, *Annu. Rev. Anal. Chem. (Palo Alto. Calif).*, 2008, **1**, 293–327.
[6] T. Ly and R. R. Julian, *J. Am. Soc. Mass Spectrom.*, 2008, **19**, 1663–72.
[7] T. Ly and R. R. Julian, *J. Am. Chem. Soc.*, 2008, **130**, 351–8.
[8] A. J. Kastin and W. Pan, *Curr. Pharm. Des.*, 2010, **16**, 3390–400.
[9] C. Janus, J. Pearson, J. McLaurin, P. M. Mathews, Y. Jiang, S. D. Schmidt, M. A. Chishti, P. Horne, D. Heslin, J. French, H. T. Mount, R. A. Nixon, M. Mercken, C. Bergeron, P. E. Fraser, P. St George-Hyslop and D. Westaway, *Nature*, 2000, **408**, 979–82.
[10] R. A. S. Santos, A. C. Simoes e Silva, C. Maric, D. M. R. Silva, R. P. Machado, I. de Buhr, S. Heringer-Walther, S. V. B. Pinheiro, M. T. Lopes, M. Bader, E. P. Mendes, V. S. Lemos, M. J. Campagnole-Santos, H.-P. Schultheiss, R. Speth and T. Walther, *Proc. Natl. Acad. Sci. U. S. A.*, 2003, **100**, 8258–63.
[11] T. Barka, *J. Histochem. Cytochem.*, 1980, **28**, 836–859.
[12] T. Wyttenbach, G. Von Helden and M. T. Bowers, *J. Am. Chem. Soc.*, 1996, **118**, 8355–8364.
[13] S. D. Pringle, K. Giles, J. L. Wildgoose, J. P. Williams, S. E. Slade, K. Thalassinos, R. H. Bateman, M. T. Bowers and J. H. Scrivens, *Int. J. Mass Spectrom.*, 2007, **261**, 1–12.
[14] R. R. Hudgins, Y. Mao, M. a Ratner and M. F. Jarrold, *Biophys. J.*, 1999, **76**, 1591–7.
[15] R. R. Hudgins, M. A. Ratner and M. F. Jarrold, *J. Am. Chem. Soc.*, 1998, **120**, 12974–12975.
[16] B. T. Ruotolo and D. H. Russell, *J. Phys. Chem. B*, 2004, **108**, 15321–15331.
[17] L. J. Morrison and V. H. Wysocki, *J. Am. Chem. Soc.*, 2014.
[18] A. E. Counterman and D. E. Clemmer, *J. Am. Chem. Soc.*, 2001, **123**, 1490–1498.
[19] C. L. Moss, J. Chamot-Rooke, E. Nicol, J. Brown, I. Campuzano, K. Richardson, J. P. Williams, M. F. Bush, B. Bythell, B. Paizs and F. Turecek, *J. Phys. Chem. B*, 2012, **116**, 3445–56.
[20] Warnke, S.; von Helden, G.; Pagel, K., *J. Am. Chem. Soc.* **2013** *135*, 1177–80.
[21] Kupser, P.; Pagel, K.; Oomens, J.; Polfer, N.; Koksch, B.; Meijer, G.; von Helden, G. J. Am. Chem. Soc. 2010 132, 2085–2093.
[22] M. Mentinova and S. A. McLuckey, *J. Am. Soc. Mass Spectrom.*, 2011, **22**, 912–921.
[23] I. K. Webb, M. Mentinova, W. M. McGee and S. A. McLuckey, *J. Am. Soc. Mass Spectrom.*, 2013, **24**, 733–43.
[24] X. Zhang and R. R. Julian, *Phys. Chem. Chem. Phys.*, 2012, **14**, 16243–16249.
[25] A. T. Iavarone, J. Meinen, S. Schulze and J. H. Parks, *Int. J. Mass Spectrom.*, 2006, **253**, 172–180.
[26] A. T. Iavarone and J. H. Parks, *J. Am. Chem. Soc.*, 2005, **127**, 8606–8607.
[27] F. Talbot, A. Rullo, H. Yao and R. A. Jockusch, *J. Am. Chem. Soc.*, 2010, 16156–16164.
[28] N. S. Green, E. Reisler and K. N. Houk, *Protein Sci.*, 2001, **10**, 1293–304.
[29] J. Seebacher, P. Mallick, N. Zhang, J. S. Eddes, R. Aebersold and M. H. Gelb, *J. Proteome Res.*, 2006, **5**, 2270–82.
[30] N. G. Hendricks, N. M. Lareau, S. M. Stow, J. A. McLean and R. R. Julian, *J. Am. Chem. Soc.*, 2014, **136**, 13363–13370.
[31] J. J. P. Stewart, *J. Mol. Model.*, 2007, **13**, 1173–213.

[32] A. A. Shvartsburg and M. F. Jarrold, *Chem. Phys. Lett.*, 1996, **261**, 86–91.

Chapter 4: Two-Step Energy Transfer Enables Use of Phenylalanine in Action-EET for Distance Constraint Determination in Gaseous Biomolecules

4.1 Introduction

Determination of the gas-phase structures of proteins and peptides is a sought-after goal in the field of mass spectrometry (MS).[1-15] One approach relies on energy transfer to reveal distance constraints that can be coupled with simulations to obtain structures. Recently, energy transfer between native residues[16] or between chemically appended groups[17] that results in a diagnostic bond cleavage have been reported, enabling facile distance constraint determination in MS based experiments. Energy transfer from native chromophores to disulfide bonds occurs with a strict distance dependence (less than ~6 Å for Tyr or ~15 Å for Trp). Combined with computational methods, this data can be used to accurately determine the gas-phase structures of proteins and peptides.[18]

Interestingly, our previous investigations did not reveal any energy transfer from phenylalanine, a weak chromophore compared to Tyr and Trp. Herein we present results where Phe is observed to transfer energy to Tyr, which then transfers energy sequentially to a disulfide bond via a two-step mechanism. Precedence for sequential energy transfer can be found in Forster Resonance Energy Transfer (FRET) literature. Two-step FRET, in which three or more chromophores participate in sequential energy transfer, has been previously characterized in solution[19-21] and successfully applied in a variety of impactful reports.[22-25]

Experiments in this study began by modifying a cysteine-containing peptide with propylmercaptan (PM) via disulfide bond formation. Excitation of a nearby chromophore causes homolytic cleavage of the disulfide and an easily detectable mass shift in the precursor ion. We call this experiment action-EET (excitation energy transfer, a collective term encompassing both FRET and Dexter exchange transfer) in analogy with action spectroscopy.[6] Experiments were conducted in a Thermo LTQ modified with a tuneable OPO laser to excite ions stored in the ion trap. Details of this setup have been described previously.[16] Photons excite the isolated peptide at varying wavelengths while loss of propylmercaptan radical is monitored. The data is compiled to yield an action-EET spectrum. Features of Tyr action spectra are well defined (see below) and make determination of Tyr-disulfide proximity straightforward. The fact that tyrosine must be within ~6 Å of a disulfide to participate in EET makes proximity determination unambiguous in even small peptides.

4.2 Experimental

Materials and synthetic details

Peptides were purchased from American Peptide Company. The peptides YF and CQDSETRTVY were synthesized by standard solid-phase procedures detailed elsewhere.

Peptides were reacted with propyl mercaptan (PM) by adding 1 µL of PM to 1 nmol of peptide in 50% dimethyl sulfoxide-water. The mixture was incubated at 40°C overnight before removing the solvent by lyophilisation.

Photodissociation (PD) yields were determined by calculating the percent product ion formed resulting from the loss of propyl mercaptan from the modified peptide. Only the homolytic disulfide cleavage was observed in any significant yield for these experiments.

18-crown-6-methanethiol was synthesized from reacting 1.6mmol of 18-crown-6-alcohol with 1.5 equivalents of tosyl chloride and 2 equivalents of pyridine in 600 µL of dichloromethane for 1 hour. 2 equivalents of potassium thioacetate and 1 mL of methanol were added and the reaction mixture was heated to 50°C for 9.5 hours. The supernatant from the reaction mixture was removed and dried under nitrogen. The product was resuspended in 2 mL of methanol and 2 equivalents of potassium carbonate were added. The mixture was reacted for 2 hours with vigorous stirring. The supernatant was removed to obtain the product. Reaction progress at each step was monitored by mass spectrometry. The subsequent product was reacted with PM using the same procedure as in the case of peptides to yield the following structure:

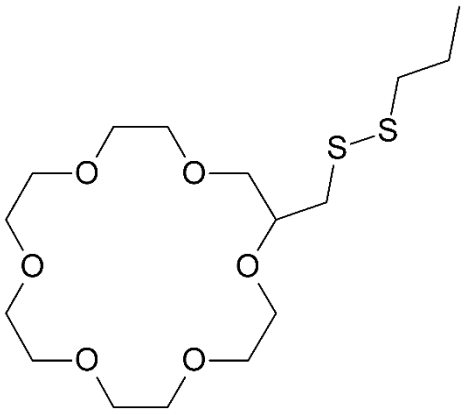

Simulated annealing molecular dynamics simulations

Simulations to obtain lowest energy structures for the examined peptides were performed according to the same methods described in [1]. Simulations were performed in the

Maestro software suite (Schrödinger Inc., Portland, Oregon). Simulations were done in 100 cycles using the OPLS 2005 force field, following with minimization using the Polak-Ribiere Conjugate Gradient (PRCG) method. Each cycle began with molecular dynamics runs were performed at 300 K (1.5 fs step interval, 1 ps duration), incrementally raising to 400, 500, and 1000 K (1.0 fs step interval, 10 ps duration) before lowering to 300 K and then 200 K (1.5 fs step interval, 10 ps duration). The structure is then minimized again by the PRCG method. Structures were saved at the end of each cycle to yield 100 structures after each simulation. Structures were subsequently sorted by energy to give the lowest-energy conformer. Constrained simulations were also performed in the same fashion, but while imposing a distance constraint between two atoms of interest (4±3 Å or 6±3 Å) to guide simulations to experimentally consistent structures. The constrained, annealed structures were then re-minimized by the PRCG method without constraints to yield a final structure and energy.

Energies were also calculated using PM6 semi-empirical calculations in the Gaussian 09 Rev A.1 software (Gaussian Inc., Wallingford, CT.). Initial structures were taken from the lowest-energy structures obtained from simulated annealing. Structures were optimized to a minimum without calculating force constants, and energies were calculated using the PM6 method in the ground state with the default spin. Charges were either +1 or +2, matching that of the CBF charge state. No counterion or solvation was present.

Disulfide dissociation energy calculations

Time dependent calculations to determine the energy of the dissociative transition for the disulfide bond were perfomed using the RB3LYP 6-31G(d) basis set in the Gaussian 09

Rev A.1 program. Energy for the dissociation of methyldisulfide was determined by finding the energy of the excited state transition from the HOMO to the LUMO (n=25 to 26), which is an antibonding orbital.

Action-EET spectra and traditional action spectra

Action spectra were compiled by monitoring (as a percent) the loss of the propyl-mercaptan radical (for action-EET) or the largest product ion (for traditional action spectra) at varying wavelengths. Average laser power levels at each wavelength were recorded. In both action-EET and traditional action spectra the relative PD yields between wavelengths were corrected according to differences in laser power.

4.3 Results and Discussion

Figure 4.1 (red trace) shows the action-EET spectrum obtained by monitoring loss of propylmercaptan from the peptide CQDSETRTFY, Collagen Binding Fragment (CBF), in the protonated 1+ charge state. The spectrum clearly shows enhanced absorption (relative to that of an isolated disulfide bond) in the 265-285 nm region which is consistent with the spectral features of Tyr (see Fig. 4.3 and 4.4, green traces for comparison). However, the two-peak absorption typical for isolated Tyr is dulled significantly. In addition, there is a new feature at 260 nm which has not been found in any previous spectra of Tyr containing peptides. Notably, CBF also contains Phe. To explore the possibility that Phe was responsible for the feature at 260 nm, we synthesized a F9V mutant. The action-EET spectrum for the F9V mutant is shown in Figure 4.1 (purple trace). The absorption feature at 260 nm is gone, suggesting that Phe is the originating chromophore for this feature. In addition, the

typical two-peak absorption for Tyr is more distinct, suggesting interaction between the chromophores. Examination of the same peptide in the 2+ charge state reveals similar trends to those observed for the 1+ charge state, including a new feature at ~260 nm that disappears in the F9V mutant (see figure 4.2).

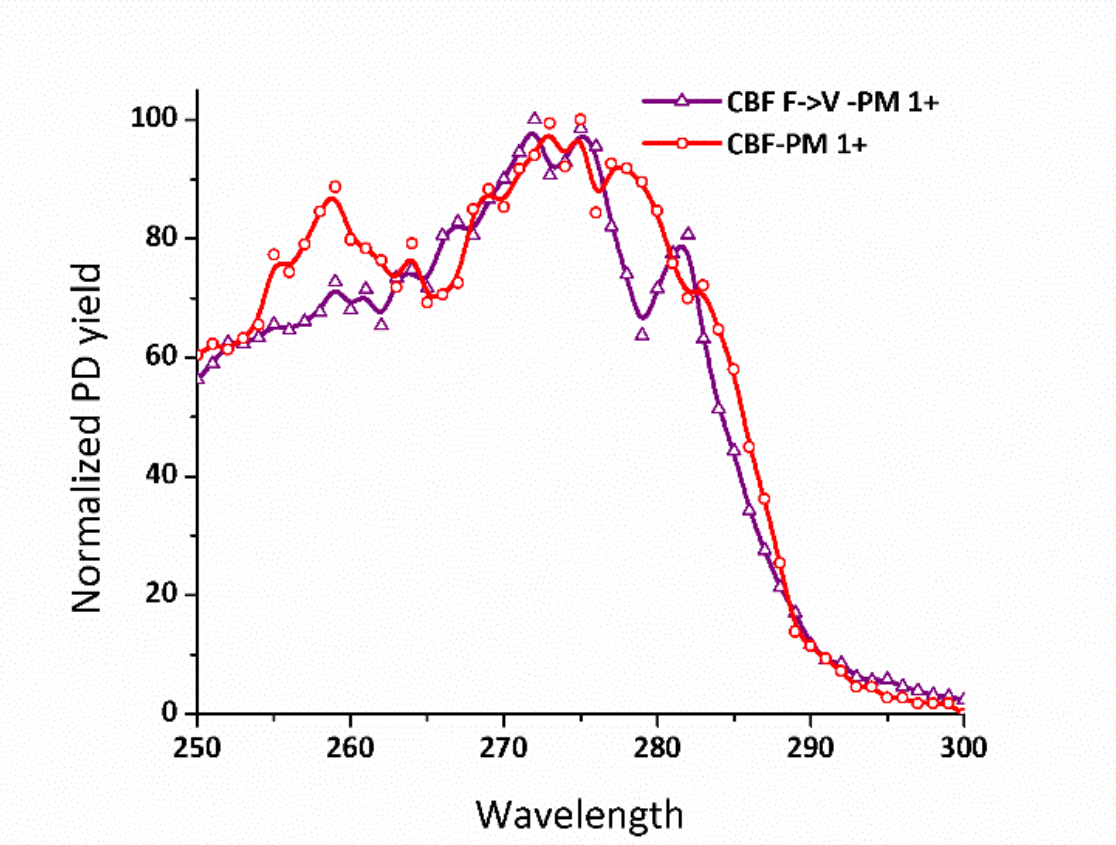

Figure 4.1. Action-EET spectra of the CBF peptide (red trace) and a F9V mutant (purple trace) in the 1+ charge state normalized to the highest PD yield in each data set.

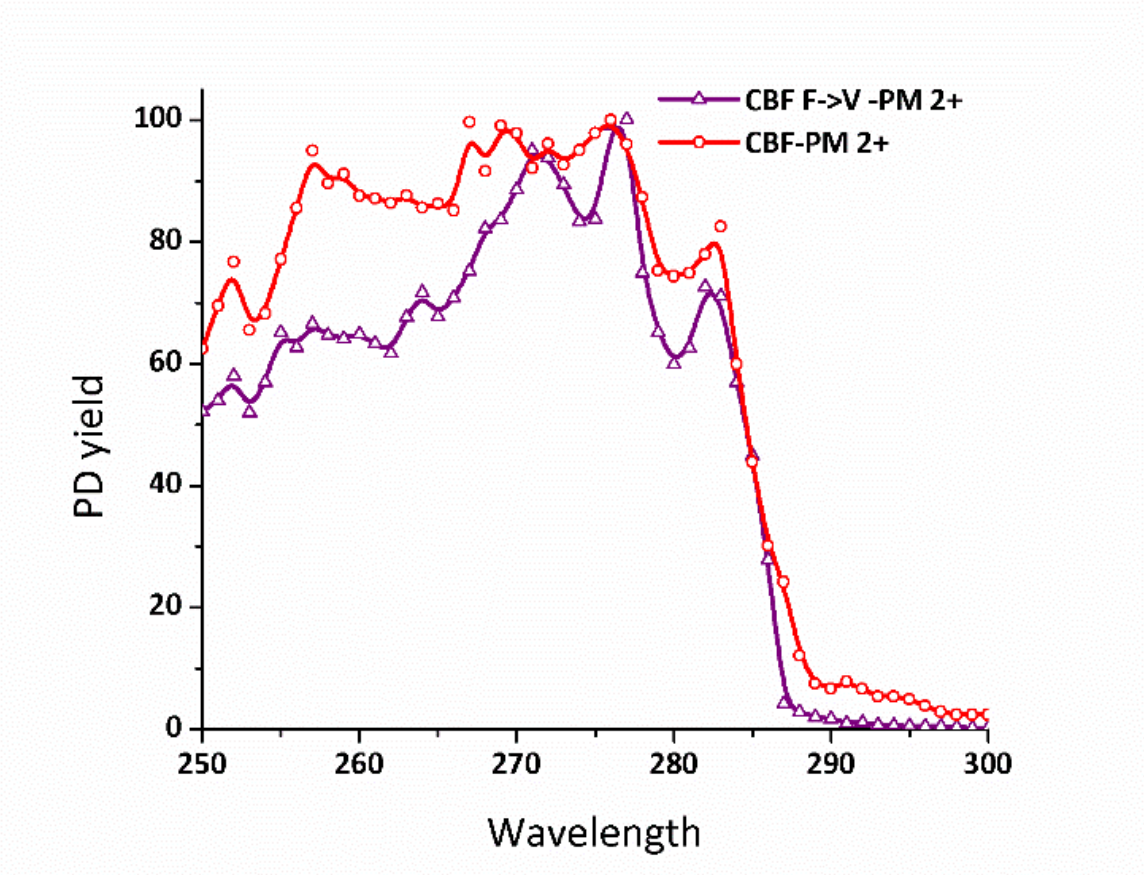

Figure 4.2. Action-EET spectra of the CBF peptide (red trace) and CBF F-to-V mutant (purple trace) in the 2+ charge state normalized to the highest PD yield in each data set.

To explore the single-step EET capabilities of Phe, we compare results for several isolated amino acids. Shown in Figure 4.2 are EET spectra for Tyr, Ala, and Phe. Each amino acid was noncovalently attached to a disulfide containing 18-crown-6 based molecule (crown-PM, see experimental for structure) that places a disulfide bond within close proximity (~4.8Å) to the side chain. The Tyr spectrum (green trace) exhibits typical features previously observed for Tyr containing peptides. In comparison, the Phe spectrum (purple trace) is featureless and has no obvious peak at ~260 nm, suggesting very minimal energy transfer, if any, occurs. To confirm that there is a lack of significant EET in the Phe

spectrum, results obtained with alanine are shown as well. The Phe and Ala spectra are very similar to each other and resemble the absorption spectrum for a disulfide bond, which is weak and featureless in this region.[16]**Error! Bookmark not defined.**

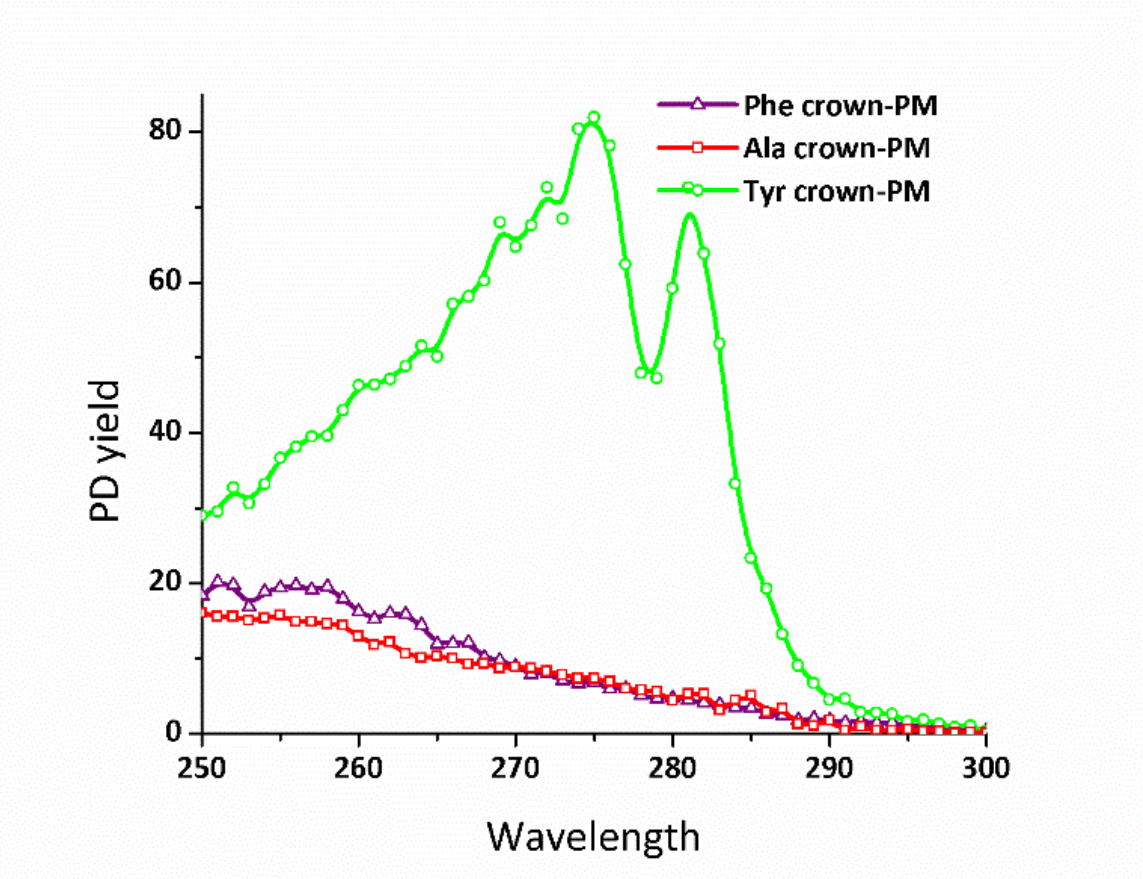

Figure 4.3. Action-EET spectra of 18-crown-6-PM noncovalently attached to Ala and Phe.

In order to determine whether Phe absorbs at 260 nm, we obtained a traditional action spectrum for the amino acid (see Figure 4.4). Absorption is most abundant at ~256 nm and rapidly declines to zero around 270 nm. This spectrum is consistent with previous spectra obtained in the gas phase.[26] There is a slight shift toward longer wavelength from the absorption maximum to the EET maximum (i.e. 256 nm → 260 nm) for Phe. This trend is consistent with the EET behavior of Tyr and Trp. This shift in wavelength may result from

stabilization of the excited state due to weak intra-molecular solvation of the chromophores. Solvation effects have been observed to lead to a bathochromic shift in solution when comparing different solvents.[27] This would also account for why there is a small amount of variability in the shift observed for different peptides (shifts are between 2-4 nm).

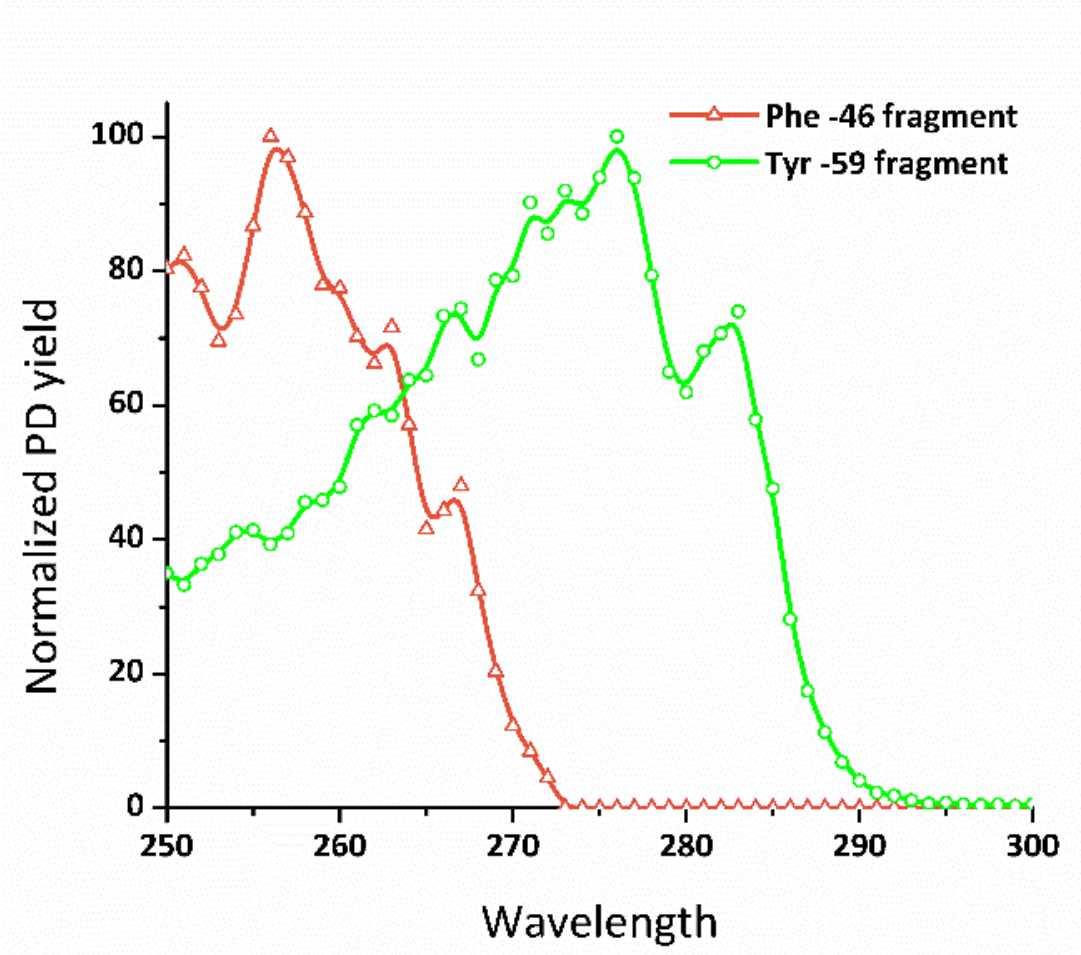

Figure 4.4. Traditional action spectra of protonated phenylalanine (orange), and tyrosine (green) showing absorption features from 250-270nm.

Taken together, the results in Figures 4.1-4 indicate that Phe is capable of EET, but only in the presence Tyr. We hypothesize that the mechanism involves two step energy transfer,

i.e. from Phe → Tyr → disulfide. Energy transfer from Phe to Tyr is feasible based on absorption/emission spectra. In the gas phase, Phe emits at 281 nm, which overlaps well with the region where Tyr absorbs (see Figure 4.4, green trace).[28] Subsequently, energy transfer from Tyr to the disulfide is well-documented.[16]

Why doesn't Phe transfer energy in a one-step process? Recently Zabuga et al reported that Phe has an exceptionally long-lived excited state in the gas phase that arises from a rapid transition to the triplet.[29] Notably, Phe is reported to remain in the excited state in excess of 100 ms whereas Tyr relaxes ~10 times faster. The long lifetime of Phe may allow it to be quenched by collisions with trace molecules in the ion trap. This would explain why Phe is normally dark in our experiments. However, the presence of a nearby Tyr residue may shorten the effective lifetime of Phe by facilitating energy transfer. There is evidence that a shortening of Phe lifetime occurs in the presence of Tyr in solution.[30]

Another explanation is that Phe emission overlaps poorly with the dissociative transition of the disulfide bond (which is predicted by theory to occur at ~342 nm, see ESI for details). Previous measurements in solution suggest that Phe emission has little or no overlap with 342 nm,[31] and is expected to have only a minor shift in transition to the gas phase. the lack of overlap may prevent EET in the absence of Tyr, which serves to bridge the gap.

Given the consistent trends that exist between all known photochemical properties of Trp, Tyr, and Phe, EET from Phe will likely occur over distances shorter than those observed for Tyr (i.e. 6 Å, since the distance dependence for Trp is longer, the trend should yield a shorter distance for Phe relative to Tyr). Based on these considerations, a conservative estimate for the EET cutoff of Phe is <~6 Å. We tested this value by examining the peptide

YF in a complex with crown-PM. In this experiment significant Phe EET is not observed (see figure 4.5). The Phe-Tyr separation cannot exceed ~8 Å for this dipeptide (based on inherent constraints due to allowable bond lengths and rotations). The lowest energy structure for this complex suggests the separation of Tyr and Phe is 7.7 Å (figure 4.6). Lack of substantive EET for YF is hence consistent with an energy cut-off inside ~6 Å.

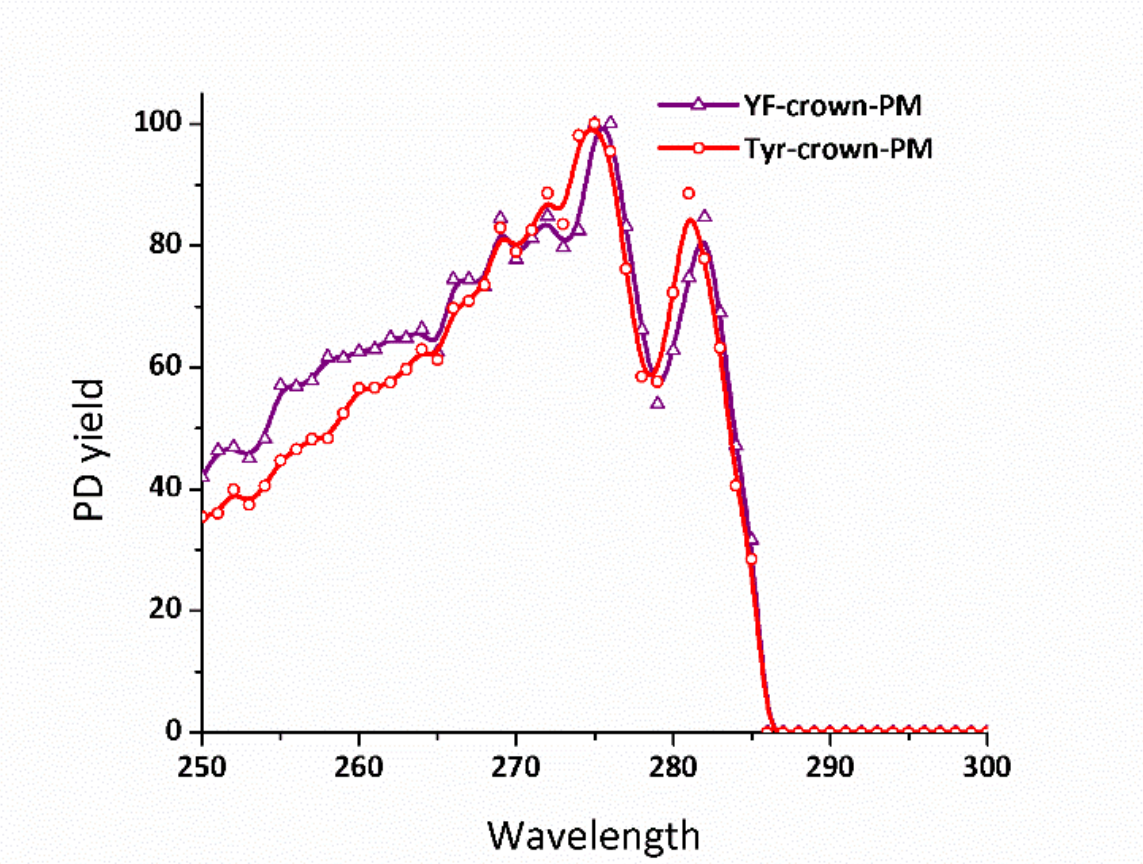

Figure 4.5. Action-EET spectra of Tyrosine (red) and the YF peptide (purple) attached to crown-PM. The red trace is representative of tyrosine absorbance spectra.

Additionally we investigated the CD36 139-155 peptide (CNLAVAAASHIYQNQFVQ) in the 2+ charge state. The action-EET spectrum showed no presence of Phe features (see figure 4.7) but the lowest energy structure for the peptide (figure 4.8), which was consistent

with Tyr energy transfer, had a Phe-to-Tyr distance of 8.0 Å, further supporting a small distance for Phe energy transfer.

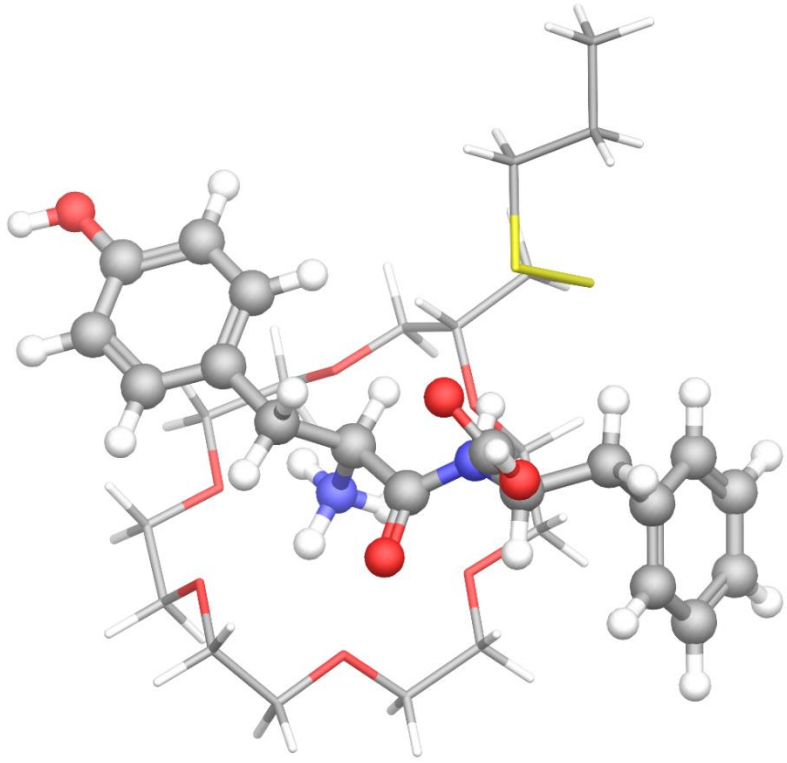

Figure 4.6. Lowest energy structure of the YF, crown-PM complex. The distance between Phe and Tyr is 7.7 Å. The simulated annealing maximum temperature was reduced to 650K (from 1000K) to preserve the noncovalent complex. All other parameters were the same as other calculations.

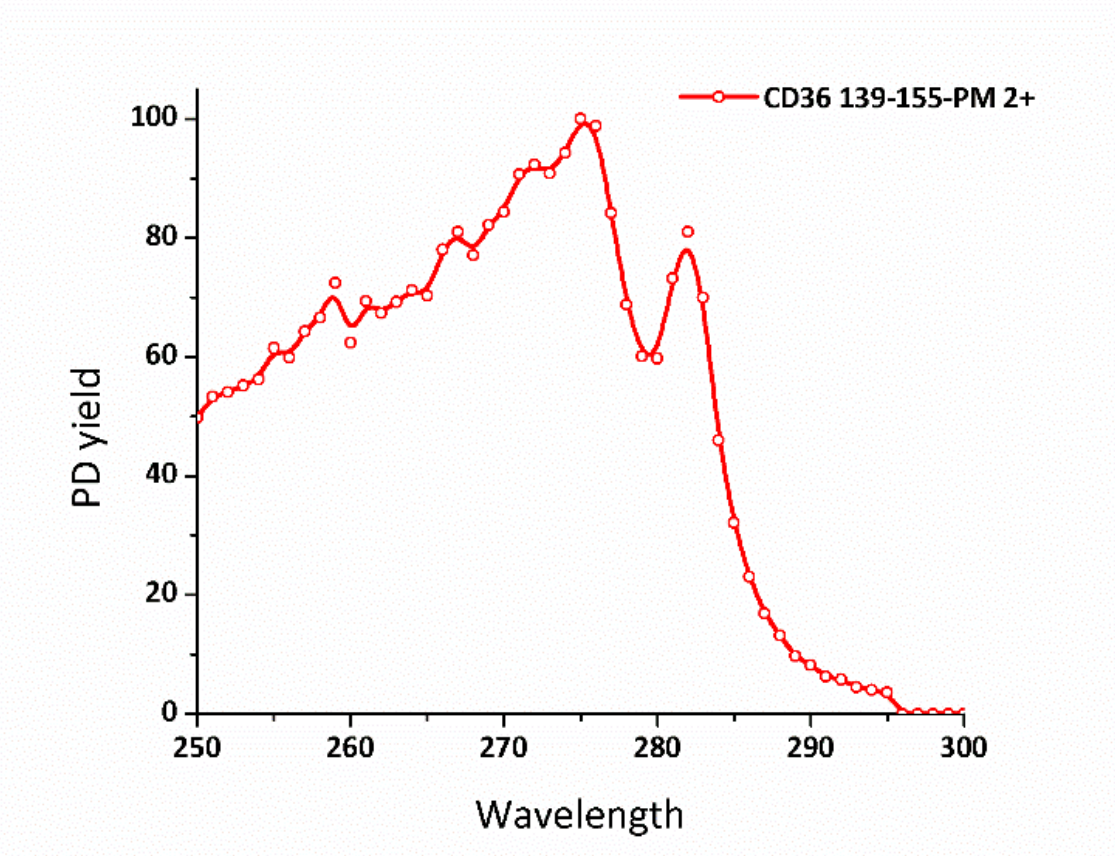

Figure 4.7. Action-EET spectrum of the 2+ CD36 139-155 peptide (CNLAVAAASHIYQNQFVQ, purchased from American Peptide Company) modified with PM.

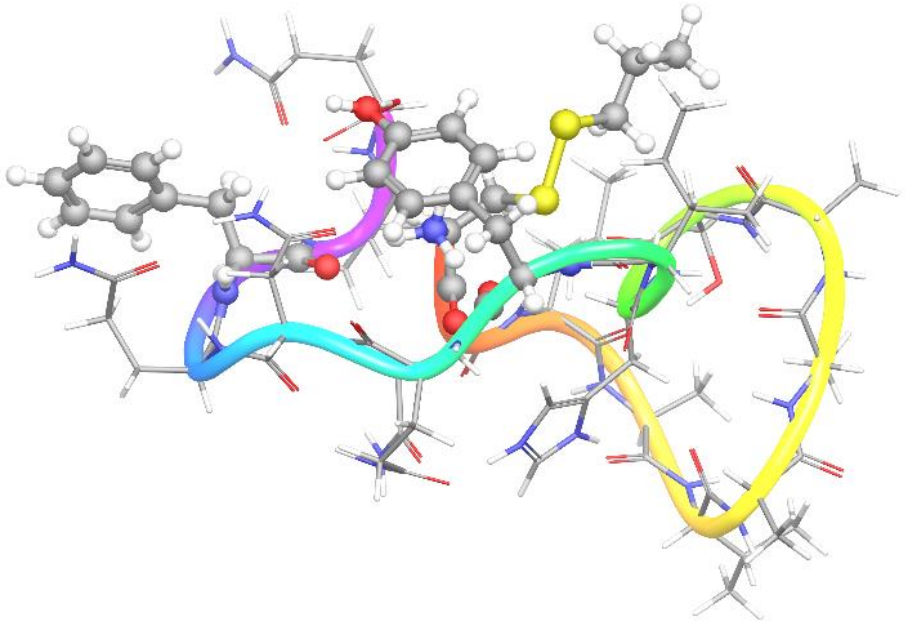

Figure 4.8. The lowest energy conformation of the CD36 139-155 peptide modified with PM (charges on N-terminus, His) as obtained by the previously mentioned simulated annealing procedure. Distance between Tyr and the disulfide is 3.6 Å, and the Phe-to-Tyr distance is 8.0 Å.

Considering the distance limitations of EET for each donor-acceptor system, the data in Figure 4.1 can be interpreted in relation to the structure of the peptide. As demonstrated previously, the Tyr absorption near ~275 nm implies that the disulfide bond is within ~6 Å of the Tyr side chain. Similarly, the feature at ~260 nm suggests the Phe and Tyr side chains are likely within ~6 Å. At room temperature the peptide can be expected to readily undergo sidechain rotations and some degree of conformational flexibility. Initial exploration of the protonated peptide structure (charged at arginine) by simulated annealing did not yield a low energy structure matching these criteria, so distance constraints were used to guide the calculations towards relevant conformational space (computational experiments are

described in greater detail in the supporting information). After re-minimization in the absence of distance constraints, the low energy structure shown in Figure 4.9 was obtained. This structure is 53 kJ/mol higher in energy than the global minimum when evaluated by the OPLS 2005 force field. PM6 Semi-empirical calculations yield an energetic difference of only 6 kJ/mol for the re-optimized structure. From these calculations it is evident that theory predicts multiple structures that are energetically equivalent. Hence the experimental distance constraints obtained through action-EET are highly valuable for identifying the correct conformation. The same simulated annealing approach was used to generate a structure for the 2+ charge state of the peptide (charges on N-terminus, arginine, Figure 4.10). In this case, the lowest energy structure is consistent with the distances expected from the action-EET data, with Phe-Tyr and Tyr-Cys distances under ~6 Å.

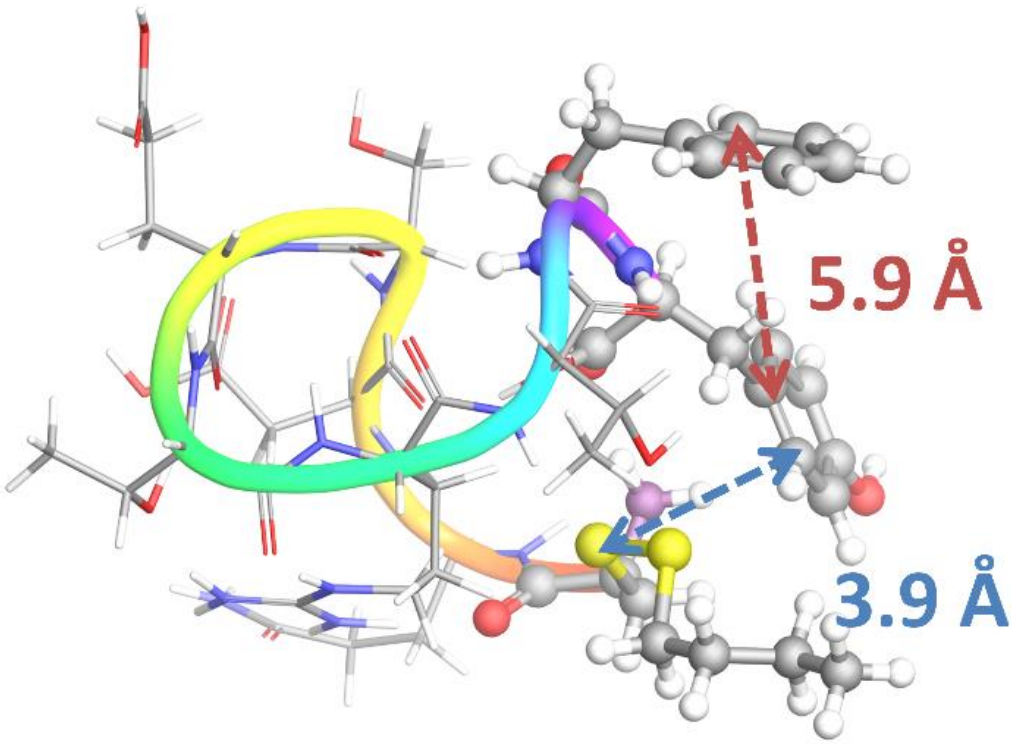

Figure 4.9. Lowest energy structure of the CBF 1+ peptide consistent with experimental data. Distances shown are Tyr-disulfide (blue) and Phe-Tyr (red).

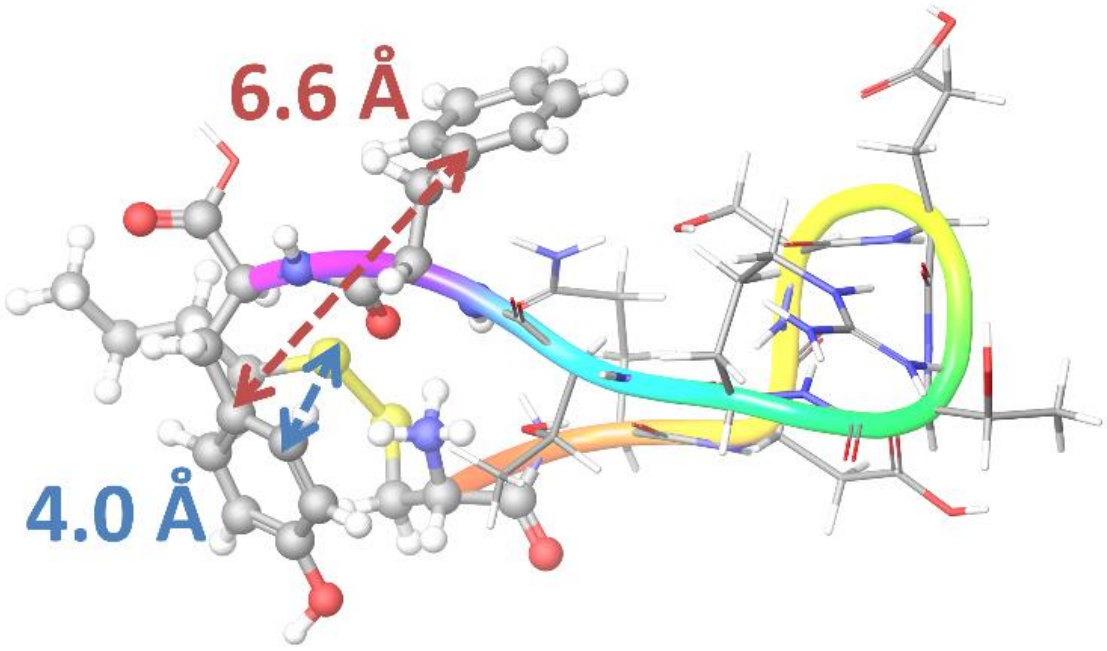

Figure 4.10. Lowest energy structure of the CBF 2+ peptide. Distances shown are Tyr-disulfide (blue) and Phe-Tyr (red).

4.4 Conclusions

In conclusion, two-step energy transfer is demonstrated in the gas phase for the first time. Although Phe is not useful in single-step action EET experiments, it can be employed in two-step action EET in combination with Tyr. It is likely that other two-step energy partners will be discovered in the future. Furthermore, two-step EET experiments simultaneously reveal two distance constraints that can be used in conjunction with calculations to accurately define peptide structure. These

experiments will help guide efforts to delineate the role of mass spectrometry in protein structure determination.

4.5 Acknowledgements

This research was supported by the National Science Foundation (CHE-1401737).

4.6 References

[1] M. Forbes, and R. Jockusch, *J. Am. Soc. Mass. Spectrom.*, 2011, **22**, 93.
[2] S. R. Harvey, C. E. Macphee and P. E. Barran, *Methods*, 2011, **54**, 454–61.
[3] N. C. Polfer, B. Paizs, L. C. Snoek, I. Compagnon, S. Suhai, G. Meijer, G. von Helden and J. Oomens, *J. Am. Chem. Soc.*, 2005, **127**, 8571–9.
[4]S. Warnke, G. von Helden and K. Pagel, *J. Am. Chem. Soc.*, 2013, **135**, 1177–80.
[5]T. Wyttenbach and M. T. Bowers, in *Modern Mass Spectrom.*, 2003, vol. 225, pp. 207–232.
[6] T. Baer and R. C. Dunbar, *J. Am. Soc. Mass Spectrom.*, 2010, **21**, 681–693.
[7]J. L. P. Benesch and C. V Robinson, *Nature*, 2009, **462**, 576–7.
[8] L. Shi, A. E. Holliday, H. Shi, F. Zhu, M. A. Ewing, D. H. Russell and D. E. Clemmer, *J. Am. Chem. Soc.*, 2014, **136**, 12702–11.
[9] A. S. Danell and J. H. Parks, *J. Am. Soc. Mass Spectrom.*, 2003, **14**, 1330–9.
[10] A. S. Danell and J. H. Parks, *Int. J. Mass Spectrom.*, 2003, **229**, 35–45.
[11] A. T. Iavarone and J. H. Parks, *J. Am. Chem. Soc.*, 2005, **127**, 8606–8607.
[12] A. T. Iavarone, J. Meinen, S. Schulze and J. H. Parks, *Int. J. Mass Spectrom.*, 2006, **253**, 172–180.
[13] A. T. Iavarone, A. Patriksson, D. van der Spoel and J. H. Parks, *J. Am. Chem. Soc.*, 2007, **129**, 6726–6735.
[14] M. Dashtiev, V. Azov, V. Frankevich, L. Scharfenberg and R. Zenobi, *J. Am. Soc. Mass Spectrom.*, 2005, **16**, 1481–7.
[15] V. Frankevich, V. Chagovets, F. Widjaja, K. Barylyuk, Z. Yang and R. Zenobi, *Phys. Chem. Chem. Phys.*, 2014, **16**, 8911–20.
[16]N. G. Hendricks, N. M. Lareau, S. M. Stow, J. A. McLean and R. R. Julian, *J. Am. Chem. Soc.*, 2014, **136**, 13363–13370.
[17] S. Daly, F. Poussigue, A.-L. Simon, L. MacAleese, F. Bertorelle, F. Chirot, R. Antoine and P. Dugourd, *Anal. Chem.*, 2014, **86**, 8798–804.
[18] N. G. Hendricks, R. R. Julian, *Phys. Chem. Chem. Phys.*, 2015, DOI: 10.1039/C5CP01617G
[19] H. M. Watrob, C. Pan and M. D. Barkley, *J. Am. Chem. Soc.*, 2003, **125**, 7336–7343.
[20] D. Kaschak, J. Lean, C. C. Waraksa, G. B. Saupe, H. Usami and T. E. Mallouk, *J. Am. Chem. Soc.*, 1999, **121**, 3435–3445.
[21] S. Kawahara, T. Uchimaru and S. Murata, *Nucleic Acids Symp. Ser.*, 1999, **42**, 241–242.

[22] M. Suresh, A. K. Mandal, E. Suresh and A. Das, *Chem. Sci.*, 2013, **4**, 2380.
[23]A. K. Tong, S. Jockusch, Z. Li, H.-R. Zhu, D. L. Akins, N. J. Turro and J. Ju, *J. Am. Chem. Soc.*, 2001, **123**, 12923–12924.
[24]I. L. Medintz, A. R. Clapp, H. Mattoussi, E. R. Goldman, B. Fisher and J. M. Mauro, *Nat. Mater.*, 2003, **2**, 630–8.
[25] H. H. Chen, Y.-P. Ho, X. Jiang, H.-Q. Mao, T.-H. Wang and K. W. Leong, *Nano Today*, 2009, **4**, 125–134.
[26]S. J. Martinez, J. C. Alfano and D. H. Levy, *J. Mol. Spectrosc.*, 1992, **156**, 421–430.
[27] M. J. Kamlet, J. L. Abboud and R. W. Taft, *J. Am. Chem. Soc.*, 1977, **99**, 6027–6038.
[28] P. Kushwaha and P. Mishra, *J. Photochem. Photobiol. A Chem.*, 2000, **137**, 79–86.
[29]A. V Zabuga, M. Z. Kamrath, O. V Boyarkin and T. R. Rizzo, *J. Chem. Phys.*, 2014, **141**, 154309.
[30] D. G. Searcy, T. Montenay-Garestier and C. Hélène, *Biochemistry*, 1989, **28**, 9058–65.
[31]F. Teale and G. Weber, *Biochem. J.*, 1957, **65**, 476–482.

Chapter 5: Concluding Remarks

5.1 Overview

Energy transfer presents a useful phenomenon for the study of structural details in biomolecules. The Action-EET system developed here makes distance-sensitive energy transfer studies more amenable to mass spectrometry. It has been demonstrated that a disulfide can act as an energy transfer acceptor from excited tyrosine and tryptophan within a Dexter energy transfer-based regime. Having characterized the distances at which these energy transfer reactions can occur, we are equipped to apply this phenomenon to the exploration of three-dimensional structure. The application of this system to numerous peptides and the Trpcage mini-protein has revealed that Action-EET and Action-EET spectra can reveal features corresponding to the hydrogen bonding environment of the donor, two-step energy transfer systems, and other highly specific information that is useful for the structural characterization of molecules.

5.2 Future Directions

The application of Action-EET to larger systems, proteins, and other molecules of interest is a target of ongoing and future work. A strength of this method is that the energy transfer donors and the precursor for the acceptor are already ubiquitous in biology, meaning that harsh, extensive modifications can generally be avoided. This is a great benefit because the integrity of the structures analyzed by this method can be relatively unperturbed. Many traditional chromophores for energy transfer are bulky, highly

hydrophobic, charge-carrying, and require harsh chemistry to modify biomolecules. While many structures have been studied in solution with these types of chromophores, whether or not such extensive modifications will have a greater impact on the transfer of structures to the gas phase remains unclear.

While a select few proteins may be ideally suited for study by Action-EET without modification beyond disulfide formation with propyl mercaptan, most will call for point-mutations to facilitate study. Recombinant DNA techniques for the production of custom protein mutants are well-established and can enable application of this method to a wide array of systems. Ongoing and future applications of Action-EET in the Julian lab will utilize this set of methodology for studying proteins.

There is also potential to utilize other avenues for introduction of a donor or acceptor into a system of interest. The crown-PM structure utilized in chapter 4 can be bound non-covalently to many structures through the amine-binding affinity of the crown ether. This allows introduction of an action-EET acceptor to a system with no chemical modification. A small amount of unpublished work has been done investigating the occurrence of energy transfer in insulin by this method. This approach of course introduces the obstacle of ambiguity in the location of the acceptor, as there are generally multiple sites that accept 18-crown-6 binding. This however remains an option for introduction of action-EET acceptors or donors, and if combined with experiments that remove the ambiguity of the crown binding site, can be a viable format for action-EET experiments.

Another avenue for future advancement of gaseous Action-EET is the exploration of additional donor-acceptor systems. There has been some investigation into modifying

established chromophores and energy transfer acceptors to yield dissociation-based reporting of energy transfer. Now that it is established that disulfides act as acceptors for energy transfer, modifying existing dyes with disulfide linkages present an opportunity to form Action-EET systems which work at varying distances or possibly by other mechanisms such as FRET.

Future investigations utilizing Action-EET will explore the structures of biomolecules such as proteins and protein complexes. This method can also serve to probe specific changes in structure that may be induced by conditions related to transfer to the gas phase.